Disordered electronic systems. II. Phase separation and the metal-insulator transition in metal-metalloid alloys

Joachim Sonntag*
HL-Planartechnik GmbH, Hauert 13, 44227 Dortmund, Germany
(Received 31 March 2004; published 23 March 2005)

The electronic transport in the phase separated regime is determined by both the different *local band structure* in the phases (called phases *A* and *B*) and *electron redistribution (electron transfer)* to the phase with the deeper average potential (phase *B*). Equations for the dependence of the electronic conductivity σ on metalloid concentration x are derived. In amorphous metal-metalloid alloys the metal-insulator transition (M-I transition) characterized by the transition from $\sigma>0$ to $\sigma=0$ at temperature $T=0$ at $x=x_c$ takes place in the phase separated regime. The M-I transition in $S_{1-x}M_x$ alloys is determined by the conduction band (phase *A*), whereas in $N_{1-x}M_x$, and in many $T_{1-x}M_x$ alloys, it is determined by the valence band (phase *B*) (*N* and *T* stand for a transition metal with completely and incompletely occupied *d* band, respectively, *S* for a simple metal as Al, Ga, In,…, and *M* for a metalloid element as Si or Ge). (1) *Granular structure*, (2) rapid decrease of the average metal grain size with increasing x, and (3) relatively small x_c are characteristic features for $S_{1-x}M_x$ thin films deposited under extreme deposition conditions and are caused by the fact that a considerable part of electrons transferred occupy surface states leading to charged phase boundaries. The *fractal* structure found in $Al_{1-x}Ge_x$ alloys after annealing is related with the formation of a maximum of phase boundary faces for acceptance of the transferred electrons. For strong scattering in a single phase, there are a minimum metallic conductivity $\sigma_{\min}\simeq(c^*/6)(e^2/h)(1/d)$ and mobility edges at density of states $4c^*m/h^2d$, where $c^*=1/4$ (d is the average atomic distance. e and m are the elementary charge and effective mass of the electrons, respectively, and $\hbar=h/2\pi$ is Plancks constant).

DOI: 10.1103/PhysRevB.71.115114 PACS number(s): 71.23.−k, 71.30.+h, 71.55.Jv, 72.15.Cz

I. INTRODUCTION

The metal-insulator transition (M-I transition) in disordered electronic systems is one of the most challenging problems in condensed matter science. "The fundamental question, still unsolved after almost half a century of intense study, is whether the electrical conductivity vanishes discontinuously…or smoothly…at the transition" (Edwards *et al.*).[1] This is immediately connected with the question of whether there exists a *minimum metallic conductivity* $\sigma_{\min}$ as originally proposed by Mott.[2,3] Today, it is generally believed that the M-I transition is *continuous* in three-dimensional systems and that there is not a $\sigma_{\min}$ in accordance with the predictions of the scaling theory of localization.[4,5] Already 2 decades ago Thouless[6] regarded "the concept of minimum metallic conductivity as one of the creative errors that helped the progress of science." For *metal-metalloid alloys* this point of view seems to be in good correspondence with experimental results.[7–9] Nevertheless, there is also support for Mott's original proposal (Möbius *et al.*[10–15]), and the existence of a $\sigma_{\min}$ is considered to be a possible scenario, when electron-electron interaction is taken into account.[1] For amorphous alloys a *random and homogeneous* distribution of the metal atoms in the amorphous matrix is often assumed, and the M-I transition is generally accepted to be a type of Anderson transition,[16–23] where the *potential disorder* plays the most important role.[24,25]

In contrast to this view, in the first part[26] of the present paper series (called Pap. I in the following), an alternative and independent discussion was presented for the metallic regime of amorphous transition-metal-metalloid alloys with the following *conclusions*.

For large ranges of concentration there is

(i) *amorphous phase separation* between two different amorphous phases called phase *A* and phase *B*, where each phase has its "own" short-range order (SRO),

(ii) the *amorphous phase separation* leads to *band separation* in the conduction band (CB) and valence band (VB) connected with the phases *A* and *B*, respectively, and the electrons are freely propagating and the corresponding *wave functions are extended* with respect to connected phase ranges, and

(iii) between the two coexisting phases there is *electron redistribution (electron transfer)* which can be described by

$$n(\zeta)=n_A\exp(-\beta\zeta), \tag{1}$$

where ζ is the quotient of the volume or atomic fractions of the two coexisting phases.[27] $n(\zeta)$ is the electron density in the phase *A* with $n_A=n(0)$. β is a constant for a given alloy, which is determined by the average potential difference between the two phases.

Conclusion (i) amorphous phase separation is now confirmed experimentally for a series of amorphous transition-metal-metalloid alloys: Edwards *et al.*[28] reported on measurements of radio frequency reactive cosputtered a-$Ni_{1-x}Si_x$:H using Raman spectroscopy, infrared absorption and extended x-ray absorption fine structure (EXAFS) that for $x>0.7$ there is indication for close-packed Si:Ni clusters beside an a-Si matrix and they speculated that the system contains two amorphous phases: one being semiconducting and the other being semi-metallic. For a-$Au_{1-x}Ge_x$ (x

>0.63) Edwards *et al.*[29] concluded from EXAFS that regions of a Ge-Au alloy are embedded in amorphous Ge host network. From small-angle x-ray scattering and x-ray-absorption near-edge spectroscopy experiments at cosputtered a-$Fe_{1-x}Ge_x$ films with $0.28<x<0.63$ Lorentz *et al.*[30] concluded phase separation into two phases likely to be a-$FeGe_2$ and a-Fe_3Ge. Applying anomalous small-angle x-ray scattering (ASAXS), Regan *et al.*[31] found in cosputtered a-$W_{1-x}Ge_x$, a-$Fe_{1-x}Ge_x$, a-$Fe_{1-x}Si_x$, and a-$Mo_{1-x}Ge_x$ films phase separated regions of the order of 1 nm in the growth plane and 1.5–2.0 nm in the growth direction. They could show that their measurements are in agreement with the assumption of two coexisting amorphous phases, a-Ge or a-Si, on the one side and a metallic phase with $FeGe_2$, $FeSi_2$, or $MoGe_3$ compositions for the last three systems, respectively, on the other side. Raap *et al.*[32] found amorphous phase separation in cosputtered a-$Fe_{1-x}Si_x$ films into regions of a-Si and an intermetallic close in composition to a-$FeSi_2$ with $\sim$0.6 nm in the film plane and $\sim$1 nm in size in the growth direction using ASAXS.

Support for the *conclusion (ii)* comes from measurements of the electronic specific heat coefficient γ of a-$Mo_{1-x}Ge_x$ (Yoshizumi *et al.*),[33,34] a-$Au_{1-x}Si_x$ (Fischer and Löhneysen),[35] a-$Vi_{1-x}Si_x$ (Mizutani *et al.*),[36] and a-$Ti_{1-x}Si_x$ (Rogatchev *et al.*):[37] γ does not go to zero at the M-I transition, but varies smoothly across the M-I transition. Support for *conclusion (ii)* comes also from the result by Abkemeier *et al.*[38,39] who found by an analysis of conductivity data in a-Ni-Si:H on the insulating side that a consistent interpretation is obtained, if it is assumed that the *wave functions of the electrons contributing to conduction are extended through clusters* of metal atoms and only localized by longer-range disorder, where the metal atoms are assumed to be Ni.

Conclusion (iii) is not yet confirmed or supported by independent authors.

The convincing confirmation and support for *conclusions* (i) and (ii) is the motivation for the present publication: purpose is a consistent description of the connection between SRO and electronic transport in metal-metalloid alloys as a basis for the description of the M-I transition. Basis for the present paper is the *amorphous phase separation model* of Pap.I with the CB and VB connected with phases A and B, respectively.

An electron moving through the alloy is *not restricted to a single phase*, but it can overcome the phase boundaries, provided both the CB and the VB are incompletely occupied. The crucial point is that in the two different phases, this electron is exposed to different local band structures (1) with different densities of states at the Fermi level (2) depending on the local band structure and the distribution of the electrons to the available electronic bands.

Applying known valence band spectra in Sec. II a microscopical model is developed for describing the electronic structure and electronic transport in metal-metalloid alloys which takes into account in particular

1. the internal surfaces (phase boundaries),
2. the average compositions of the two phases, and
3. electron redistribution (electron transfer) between the phases.

On the basis of this microscopical model, in Sec. III the effect of both the local band structure and the electron distribution between the phases on the electronic conductivity σ is considered applying effective medium theory (EMT) and the Boltzmann transport equation (BTE), and equations for the concentration dependence of σ are derived. $\sigma(x)$ closed to the M-I transition is calculated and compared with experimental results published in the literature.

In Sec. IV the application of the EMT and BTE for description of the electronic transport in disordered alloys will be justified under especial consideration of phase separation and the Ioffe-Regel criterion, and formulae for a minimum metallic conductivity and mobility edges are derived, both related to a single phase. In Sec. V the results are summarized.

II. SHORT RANGE ORDER AND ELECTRONIC STRUCTURE OF METAL-METALLOID ALLOYS

A. $N_{1-x}M_x$ and $T_{1-x}M_x$ alloys

a-Si or a-Ge represent one of the possible phases in a-$N_{1-x}M_x$, a-$T_{1-x}M_x$, and granular $S_{1-x}M_x$ alloys.[28–32,40–45] (N and T stand for a transition metal with completely and incompletely occupied d band, respectively, S for a simple metal as Al,Ga,In,…, and M for a metalloid element as Si or Ge.) Since the early 1970s it is known[46–55] that evaporated thin a-Si or a-Ge films have a heterogeneous structure characterized by density fluctuations: relatively closed packed ranges ("high density islands") are separated by ranges with smaller density ("low density channels"). The average island diameters were found to be of the order of 10 nm.[46–50,52] The high density islands have a higher degree of order in comparison with the low density channels.[49–51] During the film deposition process there is a competition between *nucleation* and *growth* of the high density islands (similar to the crystallization process in crystalline films, however, with structures without long-range order, but with a defined SRO characterized by the tetrahedral coordination typical for a-Si and a-Ge).[48] These nuclei (islands) grow until they are embedded by the neighboring grains. Now the conditions for undisturbed formation of this SRO are no longer given concerning the bonds being required angles and distances for an ideal tetrahedral bonding condition[48] and this "misfit" between the bordering islands on each other leads to the low density channels characterized by an essentially larger density of defect states (dangling bonds, vacancies, etc.). The resulting inhomogeneous structure may in fact be well described as "polyamorphous"[53] in analogy to the "polycrystalline" counterparts. According to the Davis-Mott model[56] such defects form a band of localized states near the middle of the energy gap between the valence band and the conduction band (of the *elemental* semiconductor a-M) where the Fermi level is pinned.

Regarding the formation kinetics in a-$N_{1-x}M_x$ films, e.g., a-$Au_{1-x}Si_x$, we expect an analogous situation as in a-Si films, however, with the difference that the growth of the a-Si islands is not only limited by bordering a-Si islands. The growth of the a-Si islands is also limited by the fact that there is a second atomic sort (Au) and that there can be local

fluctuations of the Au-atom distribution during the deposition process, so that also nuclei with the a-μ structure[43–45] can grow beside a-Si nuclei. Although the mobility of the atoms is small (but not zero at usual deposition temperatures), amorphous structures are expected with a formation enthalpy as small as possible, under the given conditions. So we are again led to the hypothetical free-energy diagram for a-$Au_{1-x}Si_x$ proposed by Mangin *et al.*,[43,44] already applied in Pap. I (Fig. 6 in Pap. I). According to this free-energy diagram we expect within the concentration range $0.3 \lesssim x < 1$ two different amorphous phases coexisting side by side similar to the situation in crystalline materials with intermediate phases, i.e., the metal atoms are not incorporated in a *continuous random network* during growth of the thin film, but they form (with part of the Si atoms) a second amorphous phase (phase A), which occurs in addition to the a-Si phase (phase B).

The SRO in the B phase (a-Si) corresponds to the tetrahedrally coordinated SRO in a-Si, whereas the SRO of the A phase corresponds to close-packed structure typical for metallic phases,[43] and between the two phases there are boundary faces analogous to the low density channels in a-Si, because the growth of the B-phase nuclei is disturbed approaching neighboring nuclei leading to a strong disturbance of the SRO in the boundary faces. In this, we have to distinguish two different kinds of boundary faces such between two B-phase grains, on the one hand, and those between an B-phase grain and an A-phase grain, on the other hand. In the latter case the density of defect states is expected to be essentially larger than between two B-phase grains, if the bond orbitals of the B atoms (Si) have the sp^3 hybrid configuration typical for tetrahedral atom coordination, whereas overlapping of the wave functions is rather possible between the Si atoms (with sp^3 hybrid configuration) of different grains of the same phase sort, also when the required angles and distances for an ideal tetrahedral bonding condition (for B phase) are only approximately fulfilled. Therefore, we assume that part of the Si atoms (especially those of a B phase grain which immediately border on an A phase grain—called B^* atoms in the following, Figs. 1 and 2) have s^2p^2 configuration,[57] and the p orbitals of these B^* atoms overlap with d orbitals of the metal atoms in the A phase grains and p orbitals of other B^* atoms in the immediate neighborhood. This assumption is suggested by published valence band spectra of some amorphous transition metal-metalloid alloys:

In Fig. 3 the x-ray photoemission spectra of a-$Cr_{1-x}Si_x$ alloys taken from Kobayashi *et al.*[58] are reproduced. In agreement with *conclusion (i)* and analogous to the a-$N_{1-x}M_x$ alloys, for a-$Cr_{1-x}Si_x$, a-μ, and a-Si are assumed as possible *amorphous* phases with the compositions $x_A \simeq 0.3$ and $x_B \simeq 1$.[59] The spectra in Fig. 3 can be considered as an addition of those of the two coexisting amorphous phases weightened according to their volume fractions. Between $x = 0.312$ ("Cr-31.2 at.% Si") and $x = 0.806$ ("Cr-80.6 at.% Si") there is a common single peak at the same binding energy, $E_b \simeq -9$ eV, called peak 1, the peak height increases continuously with increasing Si content and can, therefore, be assigned to the a-Si phase, since the volume fraction of the a-Si phase, v_B, increases in the same direction. In the Si spectrum, this peak 1 is, however, no longer resolved, but it is merged (fused) with a considerable density of states distribution ranging until near to the energy where the energy gap of Si begins to open. Since for the Cr containing alloys ($x \lesssim 0.806$) such a very big fraction of this density of states distribution (representing the bonding sp^3 hybrid orbitals of Si) fails (at least) in the energy range between about −5 and −8 eV, there is reason for the assumption that the states belonging to the B^* atoms ($x \lesssim 0.806$) are provided by states which in a-Si (i.e., $x \simeq 1$) would be in this energy range, and the conclusion is suggested that part of the Si atoms, very probably the B^* atoms in the B phase (a-Si), have no longer sp^3 hybrid configuration, but that the bonds are realized by p orbitals which overlap with p orbitals of neighboring B^* atoms and d orbitals of the Cr atoms (of the A phase grains) as assumed earlier. This assumption is also supported by Si Kβ emission spectra published by Tanaka *et al.*[60] of amorphous and crystalline $Ni_{1-x}Si_x$ and $Pd_{1-x}Si_x$ alloys: beside *bonding* Si p states also part of the corresponding *antibonding* Si p states lie below the common Fermi level μ (chemical potential), and they are shifted to lower energy, when the metalloid

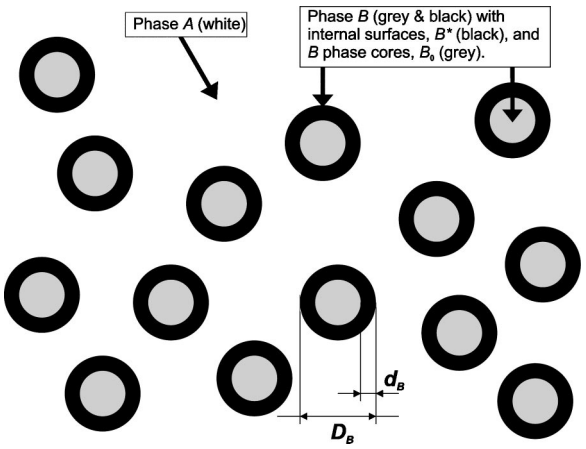

FIG. 1. Amorphous phase separation in a-$N_{1-x}M_x$ alloys for $v_B < 1/3$, where v_B is the volume fraction of the B phase. B^* characterizes the internal surfaces (monoatomic surface layers of the B-phase grains) which are assumed to have s^2p^2 configuration. B_0 characterizes the core atoms of the B phase grains assumed to have sp^3 configuration. The grain sizes are approximated by spheres with an average diameter of the order of $\simeq 1$ nm.

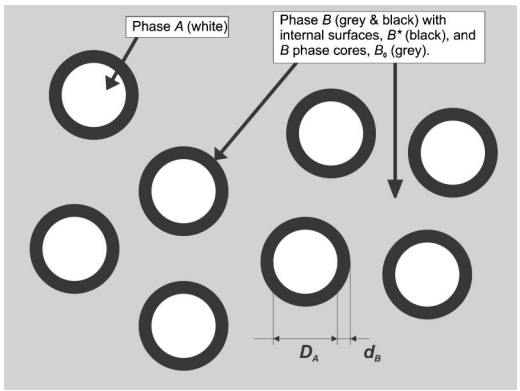

FIG. 2. Same as Fig. 1, but for $v_B > v_{B,k}$.

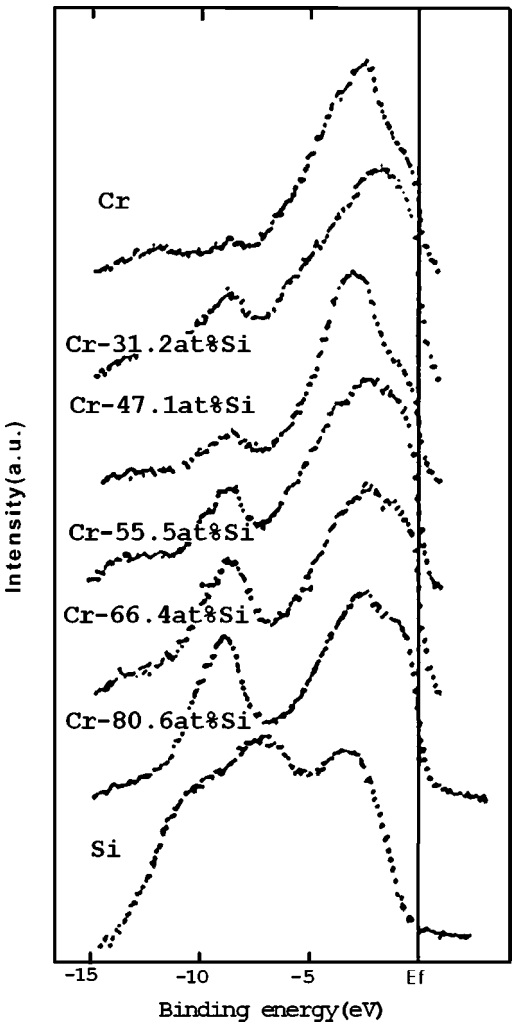

FIG. 3. X-ray photoemission spectra of a-$Cr_{1-x}Si_x$ taken from Kobayashi *et al.* (see Ref. 58).

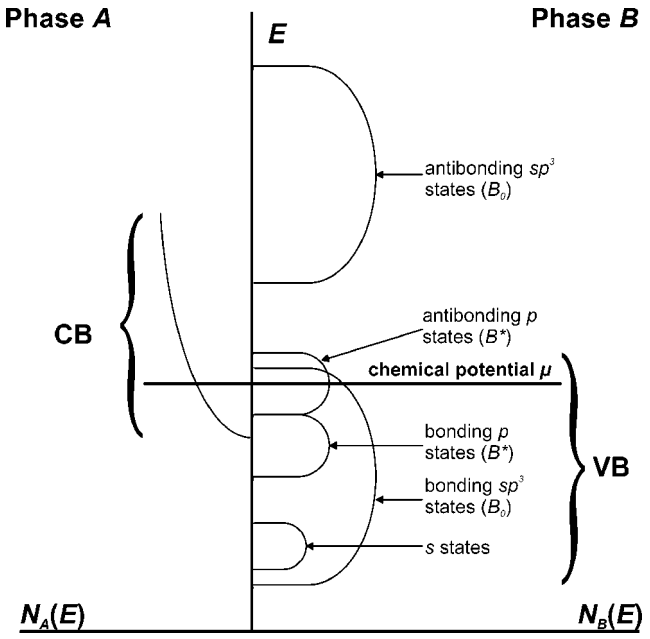

FIG. 4. Schematic band model for an a-$N_{1-x}M_x$ alloy: Densities of states $N_A(E)$ and $N_B(E)$ in dependence on energy E in the two phases A and B, phase A on the left-hand side, phase B on the right-hand side (d states or bands are not drawn). The VB consists of bonding p and antibonding p states of the mono-atomic layer of M atoms adjacent to A phase grains (B^*) and bonding sp^3 states of the atoms within the B phase cores (B_0) as drawn schematically in Figs. 1 and 2. μ characterizes the common Fermi level (chemical potential) of the alloy.

content is increased, i.e., they are partially occupied by electrons, and this occupation increases with increasing metalloid content. Regarding these spectroscopic results[58,60] and the earlier considerations, the following band sketch can be drawn for the two-phase range between a-Si (or a-Ge) and the next amorphous phase, Fig. 4. The band sketch of Fig. 4, drawn for a-$N_{1-x}M_x$ alloys, relates to a-$T_{1-x}M_x$ alloys as well, on principle, where additionally we have to take into account that the next amorphous phase (beside a-Si) can be different from a composition a-N_3M (a-μ), e.g., a-TM_3 or a-TM_2.[30–32,42] Which amorphous phases in an a-$T_{1-x}M_x$ alloy are realized, one cannot say generally, since the corresponding (equilibrium) phase diagram[61,62] only is a rough guide for possible amorphous phases with the same composition. For instance, Ishii *et al.*[40] found an amorphous $MoGe_3$ phase which has no known crystalline counterpart. On the other hand, it seems that the amorphous counterpart to the known[63,64] c-$SiCr_2$ phase is not realized[59] in the specimens by Kobayashi *et al.*[58]

From the fact that at least part of the *antibonding p* states are below the Fermi level μ,[60] the VB can be assumed to consist of bonding p and antibonding p states (from B^* atoms) and bonding sp^3 states arising from *core* atoms of the B phase grains (called B_0 atoms in the following), and that for the VB generally *hole* conductivity is expected, because both a considerable part of the antibonding p states (of the B^* atoms) and the bonding sp^3 states (of the B_0 atoms) are below μ,[60] whereas all the antibonding sp^3 states (of the B_0 atoms) are above the VB separated by an energy gap. The considerable fraction of antibonding p states below μ suggests also a considerable electron transfer from the A phase to the B phase [notice that also part of the electrons in the B phase occupy s states (of the B^* atoms) lying at energies below the bonding p states].[60] The carriers in the VB are considered to be freely propagating within connected B phase ranges as long as μ is below the top of the VB, or more precise, below the upper mobility edge of the VB (Sec. IV D).

There is an essential difference between the spectra by Kobayashi *et al.*[58] (from "Cr-31.2 at.% Si" to "Cr-55.5 at% Si") and those by Tanaka *et al.*:[60] For a-$Ni_{1-x}Si_x$ (with $x \leqslant 0.53$)[60] peak 1 assigned earlier to the a-Si phase in a-$Cr_{1-x}Si_x$ is not visible suggesting the fact that in the a-$Ni_{1-x}Si_x$ alloys, the second phase B is not a-Si, but a phase with another composition, possibly a-$NiSi_2$. A corresponding crystalline phase, c-$NiSi_2$, is known.[61–64]

Summarizing, the existence of the phase boundary faces A/B allows the acceptance of a considerable amount of additional electrons (transferred from the A phase to the B phase) in the VB: Each B^* atom provides eight electronic

states (three bonding p, three antibonding p, and two s states), whereas each B_0 atom provides only four electronic states (i.e., four bonding sp^3 states) to the VB. That is why, for a later calculation of the hole density in the VB, determination of the (atomic) fraction of the boundary face atoms B^*, X_{B^*}, is important. In the following, we have to distinguish between *volume* fractions, v_A and v_B, and *atomic* fractions, X_A and X_B, of the phases A and B, respectively. v_{B^*}, v_{B_0} are the *volume* fractions, and X_{B^*}, X_{B_0} are the *atomic* fractions taking up by the B^*, B_0 atoms, respectively.

Assuming the A and B phase grains being nearly spherical with the average diameters D_A and D_B, respectively, of the order of 1 nm, a typical value found experimentally for some a-$T_{1-x}M_x$ alloys,[32,31] then v_{B^*} and p_0^*, the available hole density in the VB without electron transfer, can be relatively large, of the order of 10^{22} cm^{-3}, as long as v_B is not too large ($v_B < 2/3$). With increasing v_B, p_0^* decreases, because v_{B^*}/v_B decreases as ζ_v increases, according to

$$\frac{v_{B^*}}{v_B} = \frac{1}{\zeta_v}\left[\left(1+\frac{2d_B}{D_A}\right)^3 - 1\right] \quad (v_B > v_{B,k}) \tag{2}$$

with

$$\zeta_v = \frac{v_B}{v_A}, \tag{3}$$

$$v_{B_0} + v_{B^*} = v_B, \tag{4}$$

$$v_A + v_B = 1, \tag{5}$$

where d_B is the average atomic diameter of the B^* atoms and

$$v_{B,k} = 1 - \left(1+\frac{2d_B}{D_A}\right)^{-3} \Big/ 3 \tag{6}$$

characterizes the volume fraction of the B phase, above it the B^* shells enveloping different A phase grains do not touch each other, see Fig. 2. For $v_B > v_{B,k}$, the fraction of the B^* atoms with s^2p^2 configuration, $X_{B^*}(v_{B^*})$, related to the fraction of the B_0 atoms with sp^3 configuration, $X_{B_0}(v_{B_0})$, decreases rapidly with increasing $X_B(v_B)$, as the sum of all the boundary faces between the phases A and B decreases rapidly as well. Because of the electron transfer from the A phase to the B phase, the true hole density, p, is still smaller than p_0^*, but decreases as well, as $X_B(v_B)$ increases, as will be studied quantitatively in Sec. III. On the other side, for $v_B < 1/3$, v_{B^*}/v_B given by

$$\frac{v_{B^*}}{v_B} = \left[1 - \left(1-\frac{2d_B}{D_B}\right)^3\right] \quad (v_B < 1/3), \tag{7}$$

is constant, if d_B/D_B is constant. For the concentration range $1/3 < v_B < v_{B,k}$, v_{B^*}/v_B is expected to decrease generally with increasing v_B or ζ_v, although it is difficult to give a quantitative relation, since part of the B surface atoms contact to each other having the sp^3 orbital configuration (B/B phase boundary faces).

A *hole* contribution of the VB to the electronic transport (at $T=0$) can only occur, when at least the common Fermi level μ still lies energetically below the upper mobility edge in the VB (Sec. IV D) corresponding to a critical hole density p_{crit}. Summarizing, the concentration dependence of p_0^* accompanied with the electron transfer leads to the fact that the hole density in the VB, p, decreases generally with increasing v_B.

Between a-Si or a-Ge and the amorphous *alloys* there is still another essential structural difference: In thin a-Si or a-Ge films the high dense islands often are grown through the whole film, i.e., there is a preferred direction perpendicular to the substrate leading to grains similar to rods (columnar structure),[51,52] because the growth of the phase grains into the perpendicular direction against the substrate is generally not hindered by other phase grains; for energetic reasons the probability that hit atoms arrange rather to the already available, growing phase grains is larger than forming new nuclei. On the other hand, in the *amorphous alloy* the appearance of the second atomic sort disturb the growth of the phase grains into all directions, and it needs diffusion processes for growth of the phase grains which, however, are strongly depressed. Therefore, in amorphous alloys, phase grains with a spherical-similar structure are expected rather than a columnar structure as in a-Si or a-Ge.

The considerations to a-$N_{1-x}M_x$ and a-$T_{1-x}M_x$ alloys can be applied, on principle, to *crystalline* or *partially crystalline* $N_{1-x}M_x$ and $T_{1-x}M_x$ alloys as well. The differences are: the realized energetic state is generally lower and the mean free paths of the carriers are generally larger in a *crystalline* phase than in an *amorphous* one. Also the average (crystalline) phase grain sizes are expected to be larger and, therefore, (v_{B^*}/v_B) is smaller for a given ζ_v leading to smaller hole densities p_0^* (and p, Sec. III B). The question of which kind of crystalline phases will be realized depends on different factors in a complex manner, where the free-energy difference between the amorphous and crystalline state and the activation energies for diffusion play an essential role. Considering a-Au-Si, a-Au-Ge, and a-Ag-Ge thin films, during annealing, first, (crystalline) Au or Ag precipitations[43,44,65,66] occur beside an a-Si or a-Ge phase, which crystallize as well, if the annealing temperature is sufficiently high leading to a phase mixing between c-Si or c-Ge and c-Au or c-Ag.[61,62]

B. $S_{1-x}M_x$ alloys

For $S_{1-x}M_x$ alloys the situation is comparable with those in $N_{1-x}M_x$ and $T_{1-x}M_x$ alloys, but with the following differences.

(1) A metastable phase with a composition S_3M corresponding to the μ phase in a-$N_{1-x}M_x$ alloys is not known in $S_{1-x}M_x$ alloys and it seems that the phases $S(M)$ and $M(S)$[67] do play the crucial role,[68] where $S(M)$ and $M(S)$ means that M atoms are solved in an S matrix, and S atoms are solved in an M matrix, respectively. $S(M)$ is the metallic phase, whereas $M(S)$ is the semiconducting (insulating) phase. Deep on the metallic side the $S(M)$ phase is generally found to be crystalline[67,69–73] and the mean free path in the phase A, L_A, is expected to be significantly larger than the average atomic distance in the metallic phase, d, whereas for

a-$N_{1-x}M_x$ and a-$T_{1-x}M_x$ alloys $L_A \simeq d$ is conjectured in the phase A for $x > 0.3$ [in analogy to the example a-$(AgCu)_{1-x}Ge_x$].[74]

(2) If each S atom solved in the $M(S)$ matrix (B phase) has the same sp^3 hybrid configuration as the M atoms as well, then each solved S atom provides *one* additional state for acceptance of *one* electron (transferred from the A phase to the B phase), provided all the sp^3 orbitals overlap with sp^3 orbitals of neighboring M or S atoms [in the $M(S)$ matrix] This condition can, however, only be fulfilled for the B_0 atoms (Figs. 1 and 2), whereas for the phase boundary atoms, B^*, there are ν orbitals per B^* atom, for which an overlap with another sp^3 orbital is not possible, and the corresponding states are not available for the VB. ν is of the order of 1.

(3) In $S_{1-x}M_x$ alloys there are no d states and therefore no d-p-orbital bonds realizing chemical bond between atoms of the different phases are possible as in $N_{1-x}M_x$ and $T_{1-x}M_x$ alloys. Therefore, in $S_{1-x}M_x$ alloys the boundary faces between phase grains of the *different* phases are assumed to be characterized by the transition from the tetrahedrally coordinated SRO with sp^3 hybrid orbitals [phase $B=M(S)$] to the close-packed structure typical for metallic phases with s^2p orbitals[57] [phase $A=S(M)$].

III. ELECTRONIC TRANSPORT AND THE M-I TRANSITION IN METAL-METALLOID ALLOYS

A. General considerations

If phase separation is realized, the electronic transport and the M-I transition *cannot be described by a model which assumes a random and homogeneous distribution of the metal atoms in a disordered matrix*. Instead, *conclusion (i)* (Sec. I) for amorphous transition-metal-metalloid alloys suggests the fact that the M-I transition at temperature $T=0$ takes place due to percolation of a *metallic* component embedded in an *insulating* component.[29,31,40] Edwards *et al.*[29] concluded from structural studies of a-Au-Ge alloys, application of percolation theory is more appropriate than the Anderson delocalization approach. On the other hand, because of *conclusion (ii)* (Sec. I), both the CB and the VB can simultaneously contribute to the electronic transport, if they are incompletely occupied. If so, and if the VB is still incompletely filled beyond the percolation threshold with respect to the A phase, then the M-I transition at $T=0$ in disordered metal-metalloid alloys with phase separation cannot be described due to percolation of a metallic component embedded in an insulating component, but another theory is necessary, which considers separately the electronic transport properties in each of the two phases A and B.

If in a disordered alloy with phase separation both the CB and the VB are incompletely occupied, then an electron moving through the alloy is *not restricted to a single phase*, but it can overcome the phase boundaries as well. The crucial point is the fact that this electron is exposed to different local band structures (1) with different densities of states at the Fermi level (2), depending on the kind of phase (A and B) and filling of the available electronic bands. The local density of states in the two phases A and B, $N_A(E)$ and $N_B(E)$, respectively, at the common Fermi level are to be assumed, generally, as different from each other, Fig. 4. While the band structure (1) in a phase determines the behavior of this electron which can be described by the concept of the effective mass, the densities of states (2) determine the current densities under the influence of an electric field. In this view it is possible to assign "own" transport coefficients to each of the two phases, σ_A, α_A, $\kappa_{e,A}$, and $R_{H,A}$ for the phase A, and σ_B, α_B, $\kappa_{e,B}$, and $R_{H,B}$ for the phase B where σ_i, α_i, $\kappa_{e,i}$, and $R_{H,i}$ are the specific conductivity, the Seebeck coefficient (thermoelectric power), the electronic contribution to the specific thermal conductivity, and the Hall coefficient for the phase i ($i=A,B$). And, if the transport coefficients σ_i, α_i, $\kappa_{e,i}$, and $R_{H,i}$ for the phases are given, then the electronic transport coefficients of disordered alloys with phase separation can be described applying the EMT. For the specific electrical conductivity σ let us apply Landauer's[75] EMT formula

$$v_A \frac{\sigma_A - \sigma}{\sigma_A + 2\sigma} + v_B \frac{\sigma_B - \sigma}{\sigma_B + 2\sigma} = 0, \tag{8}$$

which holds for nearly spherical grains of the two phases A and B. If the prerequisites for application of both the EMT equation and the BTE are fulfilled, it follows for the two phases A and B:

$$\sigma_A = \frac{e^2 h^3 L_A}{24\pi m_A^2} N_A^2(E_{F,A}) \quad \text{for} \quad v_A > \frac{1}{3}, \tag{9}$$

$$\sigma_B = \frac{e^2 h^3 L_B}{24\pi m_B^2} N_B^2(E_{F,B}) \quad \text{for} \quad v_B > \frac{1}{3}, \tag{10}$$

and for nearly free electrons [NFE approximation]

$$\sigma_A = C L_A n^{2/3} \quad \text{for} \quad v_A > \frac{1}{3}, \tag{11}$$

$$\sigma_B = C L_B p^{2/3} \quad \text{for} \quad v_B > \frac{1}{3}, \tag{12}$$

with

$$C = 2\left(\frac{\pi}{3}\right)^{1/3}\left(\frac{e^2}{h}\right). \tag{13}$$

The question of whether and under which conditions the EMT, BTE and NFE approximation can be applied, will be discussed in Secs. IV A and IV B.[76] $E_{F,i}$, L_i, and m_i are the Fermi energy, the mean free path, and the effective mass of the carriers in the phase i, respectively. e and h are the elementary charge and Planck's constant, respectively. Equations (9)–(12) hold as long as the phases A and B form infinite clusters through the sample corresponding to $v_A > 1/3$ and $v_B > 1/3$, respectively, as follows from Eqs. (8) and (5). If the phase B does not form an infinite cluster through the whole sample ($v_B < 1/3$), then in the B phase grains discrete electronic states are expected with finite energy distances, i.e., electronic transport through the B phase grains occurs by *tunneling* of electrons (temperature $T=0$), provided $\sigma_A > 0$. Analogously, the same is true for the A phase grains, if they do not form an infinite cluster through the sample (v_A

$<1/3$ and $\sigma_B>0$). That is why, the M-I transition is decisively determined by the VB, if the M-I transition occurs at $\upsilon_A<1/3$. In this case, the resulting *tunneling* conductivity in the *A* phase, σ'_A, is "*metallic*" (i.e., $\sigma'_A>0$ at $T=0$), as long as there are freely propagating carriers in the *B* phase (corresponding to a *metallic* conductivity in the *B* phase, $\sigma_B>0$ at $T=0$). Only at disappearance of the *metallic* conductivity in the *B* phase ($\sigma_B=0$ at $T=0$), σ'_A disappears as well at $T=0$ because of the additional charging energy of the electrons necessary to be overcome, i.e., for tunneling through an *A* phase grain, activation becomes necessary ($\sigma'_A>0$ only for $T>0$, if $\sigma_B=0$ at $T=0$). The situation is analogous to those in cermets or granular metals (Abeles *et al.*).[77–79] In other words, if the M-I transition in alloys with phase separation takes place in the *B* phase, the M-I transition in the *A* phase takes place *simultaneously* (at the same concentration) with the M-I transition in the *B* phase, if the *A* phase grains are separated from each other (i.e., $\upsilon_{A,c}<1/3$; $\upsilon_{A,c}=1-\upsilon_{B,c}$; $\upsilon_{B,c}$ is the volume fraction of the *B* phase at the M-I transition).

B. $N_{1-x}M_x$ alloys

Now let us calculate the hole density in the VB, *p*, in dependence on concentration. In the phase separated range of an $N_{1-x}M_x$ alloy, *p* is given by

$$p = p_0^* - \Delta n - p_{\mathrm{loc}} \tag{14}$$

with

$$p_0^* = p_0 - n_B, \tag{15}$$

where n_B is the own electron density in the *B* phase (i.e., without electron transfer),

$$n_B = \mathcal{N}_B[(1-x_B)Z_N + x_B Z_M], \tag{16}$$

and p_0 is the theoretically possible density of states available in the VB (i.e., hole density, if all the electrons in the VB are removed). p_{loc} represents the *loss* of density of states in the VB due to dangling bonds and other structure defects between touching *B* phase grains and within the cores of the *B* phase grains (B_0). Z_N and Z_M are the valences of the *N* and *M* atoms, respectively, i.e., the number of *s* and *p* valence electrons per *N* or *M* atom which are provided into the CB and VB. Δn is the increase of the electron density in the phase *B* due to electron transfer to the phase *B*, given by

$$\Delta n(\zeta_\upsilon) = \frac{n_A - n(\zeta_\upsilon)}{\zeta_\upsilon}, \tag{17}$$

with

$$n_A = \mathcal{N}_A[(1-x_A)Z_N + x_A Z_M]. \tag{18}$$

In the equations Z_N (as Z_M as well) is assumed to be invariable in the two phases. $\mathcal{N}_A$ and $\mathcal{N}_B$ are the atomic densities of the phase *A* and phase *B*, respectively. $n(\zeta_\upsilon)$ is the electron density in the phase *A* and ζ_υ is related with the *atomic* fractions of the phases *A* and *B*, X_A and X_B, respectively, by

$$\zeta_\upsilon = \frac{\upsilon_B}{\upsilon_A} = \frac{(X_B/X_A)}{(\mathcal{N}_B/\mathcal{N}_A)} \tag{19}$$

and

$$\frac{X_B}{X_A} = \frac{x - x_A}{x_B - x}. \tag{20}$$

x, x_A, and x_B are the *atomic* concentrations of the *M* atoms in the alloy, the phase *A* and the phase *B*, respectively. Applying the microscopical model described in Sec. II A, p_0, is given by

$$p_0 = 4\mathcal{N}_B\left[x_B\left(1+\frac{X_{B^*}}{X_B}\right) + \frac{\kappa}{4}(1-x_B)\right]. \tag{21}$$

Assuming $\mathcal{N}_B$ is uniform in the whole *B* phase, then

$$X_{B^*}/X_B = \upsilon_{B^*}/\upsilon_B, \tag{22}$$

and p_0 can be calculated by means of Eqs. (2), (7), (21), and (22) for $\upsilon_B>\upsilon_{B,k}$ and $\upsilon_B<1/3$, respectively (spherical phase grains). The second term in Eq. (21) takes into account the *N* atoms solved and assumed to be evenly distributed in the *B* phase, where each solved *N* atom provides κ states to the VB. Since the *N* atoms provide generally deep lying impurity levels deep in the energy gap, $\kappa=0$ can be assumed. With the equations derived we have now the possibility of calculation of the concentration dependence of the conductivity close to the M-I transition on the metallic side, at $T=0$, where it is to be considered that the electronic conductivity through the *A* phase grains takes place by tunneling, as $\upsilon_A<1/3$, as will be seen later. In the mind of Sec. III A let us apply Eq. (8), where σ_A is replaced by σ'_A, the *tunneling conductivity* through the *A* phase grains, and we get for the total conductivity σ

$$\sigma_B\frac{(3\upsilon_B-1)}{2} \leqslant \sigma \leqslant \sigma_B, \tag{23}$$

since

$$0 \leqslant \sigma'_A \leqslant \sigma_B, \tag{24}$$

i.e., the *tunneling conductivity*, σ'_A, cannot be larger than σ_B. And considering Eqs. (1), (2), and (12)–(23), the upper and lower limit for σ given by Eq. (23), can be calculated for $\upsilon_B>\upsilon_{B,k}$, Eq. (6), for the case of spherical phase grains.

The equations derived hold, on principle, for *crystalline* or *partially crystalline* $N_{1-x}M_x$ alloys as well, where it is to be considered additionally, that (1) the mean free path is generally significantly larger than the average atomic distance, if the phase considered is crystalline, and (2) the two-phase range is extended between *c*-*N* (= *A* phase) and *c*-*M*(*N*) (= *B* phase)[61,62] or between *c*-*N* and *a*-*M*(*N*),[43,44,65,66] where *M*(*N*) means that *N* atoms are solved in an *M* matrix.

a-$Au_{1-x}Ge_x$ alloys

Figure 5 shows for *a*-$Au_{1-x}Ge_x$ alloys the calculated $\sigma(x)$ dependence in comparison with experimental σ data at $T=0$, $\sigma(0\ \mathrm{K})$, and at $T=1.5$ K, $\sigma(1.5\ \mathrm{K})$, taken from Dodson

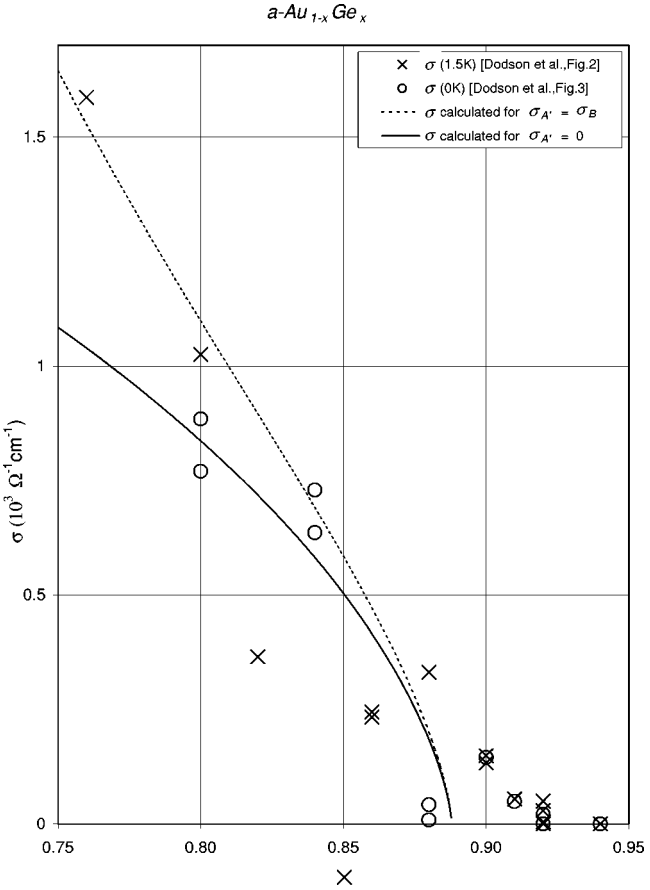

FIG. 5. Calculated $\sigma(x)$ dependence close to the M-I transition for a-$Au_{1-x}Ge_x$ and comparison with experimental data taken from Dodson *et al.* (see Ref. 66) (flash evaporation); the two calculated $\sigma(x)$ curves are the upper and lower limit for σ given by Eq. (23), where σ_B is calculated by Eq. (12) in connection with Eq. (14) and Eqs. (1), (2), and (15)–(22).

et al.,[66] Figs. 3 and 2 therein, respectively. For the calculations the following physical parameters were applied: $\mathcal{N}_A = 5.8\times10^{22}\,\mathrm{cm}^{-3}$, $\mathcal{N}_B = 5.0\times10^{22}\,\mathrm{cm}^{-3}$, $d_B = 0.244$ nm, $\beta_v = 0.8$,[27] $L_B/d_B \simeq 1$, $x_A = 0.25$, $x_B = 0.92$, $Z_N = 1$, $Z_M = 4$, $D_A \simeq 1.8$ nm, and $p_{\mathrm{loc}} \ll p$. From Eqs. (6), (19), and (20) it follows $\upsilon_{B,k} = 0.84$ corresponding to an atomic concentration of $x_k = 0.80$, i.e., for $x \lesssim x_k = 0.80$ the σ are calculated a little too big, because $\upsilon_{B^*}/\upsilon_B$ calculated by Eq. (2) is too large. The calculations provide $\upsilon_{B,c} = 0.96$ corresponding to $x_c = 0.89$, the concentration of the M-I transition. As can be seen in Fig. 5, there are some samples with $x > x_c$ which are still *metallic* apparently in contradiction to our calculations. This apparent contradiction can, however, be pretended by fluctuations regarding phase grain size and concentration, as will be discussed later. Moreover, the occurrence of additional small Au clusters beside the two phases found by Edwards *et al.*[29] for a-$Au_{1-x}Ge_x$ films can, possibly, lead to additional differences between calculation and experiment, although in the samples of Dodson *et al.*[66] (deposited at lower substrate temperature compared with those of Ref. 29) no gold clusters larger than 1 nm were found.

The applied $\mathcal{N}_A$ and $\mathcal{N}_B$ parameters are estimated from experimental atomic density data taken from Mangin *et al.*[43] for the related system a-Au-Si; $x_A \simeq 0.25$ is the average composition of the μ phase[43,44] and corresponds to a metalloid content typical for relatively stable glassy metals (Nagel,[80] Johnson and Williams[81]). d_B is set equally to the atomic diameter of the Ge atoms in c-Ge. The applied values for β_v (Ref. 82) and L_B/d_B are got by comparison with other related amorphous alloys to be studied in a separate paper. Although the value for β_v is only a rough estimate, the calculated $\sigma(x)$ dependence shown in Fig. 5 is relatively insensible against this parameter, because only the concentration range close to the M-I transition is considered. Also the value of $x_A = 0.25$ has only a very small effect to the result. In Fig. 5, defect states in the B phase were neglected (i.e., $p_{\mathrm{loc}} \ll p$). Consideration of these defect states, the curves in Fig. 5 would be shifted in direction to the x axis to smaller σ.

C. $T_{1-x}M_x$ alloys

The equations derived can be applied to $T_{1-x}M_x$ alloys as well, if Z_N in Eqs. (16) and (18), is replaced by Z_T, the valence of the T atoms, where, however, additional uncertainties come from the facts that Z_T is not known, generally, and it is to be attended that the electron redistribution includes the d electrons as well. Moreover, Z_T can be different in the two phases because of the existence of the incompletely occupied d band. Because of the d band influence, Eq. (17) is expected to be modified for $T_{1-x}M_x$ alloys. In spite of this uncertainty the M-I transition can be described by the above formulae, since in the concentration range close to the M-I transition, Δn is relatively insensible against β_v. Another difference to $N_{1-x}M_x$ alloys is the fact that additional phases are possible in $T_{1-x}M_x$ alloys (Sec. II), i.e., for description of the M-I transition, x_A can be essentially larger than in a-$N_{1-x}M_x$ alloys.

a-$Cr_{1-x}Si_x$ *alloys*

Figure 6 shows two calculations for the $\sigma(x)$ dependence for a-$Cr_{1-x}Si_x$ alloys with different assumed values for the average phase grain size, $D_A = 1.7$ and 2.3 nm. The system a-$Cr_{1-x}Si_x$ is especially interesting, since it can be considered as an example system for which, on the one hand, there are relatively many experimental data in the scientific literature, and, on the other hand, there are a series of theoretical studies with contrary results. In this connection let us recall at the controvers discussion by Okuma *et al.*[9] and Möbius[83] concerning the different experimental results in comparison to Möbius[15] and their different interpretations (see also Sec. IV C). As already argued in Sec. II, for a-$Cr_{1-x}Si_x$ the two assumed *amorphous* phases are: a-μ (phase A) and a-Si (phase B).[59] For the calculations the following physical parameters were applied: $\mathcal{N}_A = 7.9\times10^{22}\,\mathrm{cm}^{-3}$, $\mathcal{N}_B = 5.0\times10^{22}\,\mathrm{cm}^{-3}$, $d_B = 0.234$ nm, $\beta_v = 0.5$, $L_B/d_B \simeq 1$, $x_A = 0.25$, $x_B = 0.90$, $Z_{\mathrm{Cr}} = 0.5$, $Z_{\mathrm{Si}} = 4$, $p_{\mathrm{loc}} \ll p$. From Eqs. (6), (19), and (20) it follows for $D_A = 1.7$ nm and $D_A = 2.3$ nm, $\upsilon_{B,k} = 0.84$, and $\upsilon_{B,k} = 0.81$ corresponding to $x_k = 0.75$ and $x_k = 0.72$, and from the calculated $\sigma(x)$ curves in Fig. 6, $\upsilon_{B,c} = 0.97$ corresponding to $x_c = 0.87$, and $\upsilon_{B,c} = 0.91$ corresponding to $x_c = 0.81$, respectively.

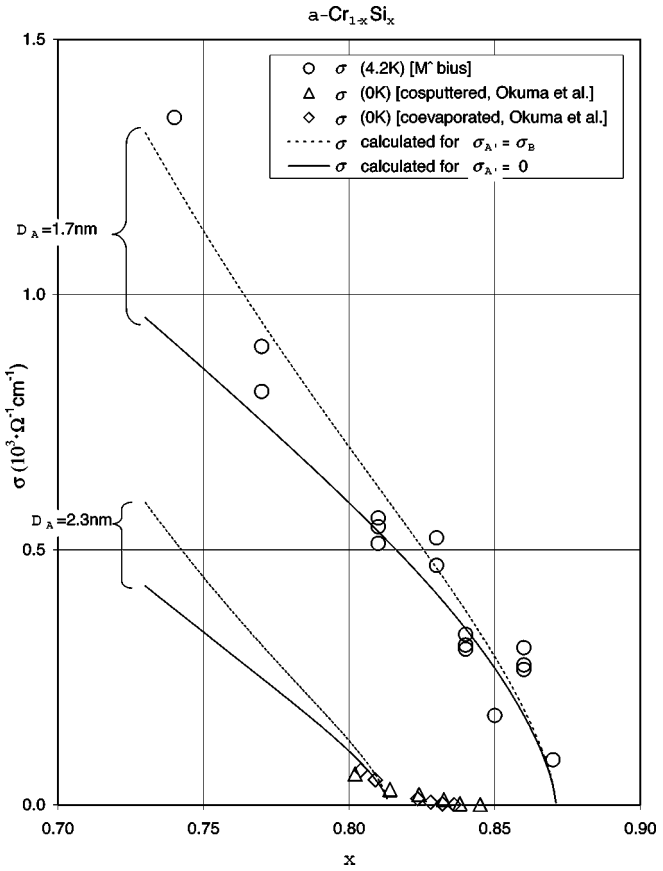

FIG. 6. Same as Fig. 5, but for a-$Cr_{1-x}Si_x$; comparison of the calculated $\sigma(x)$ dependence with experimental data taken from Möbius (see Ref. 15) (electron-beam evaporation) and Okuma *et al.* (see Ref. 9) (coevaporation and cosputtering).

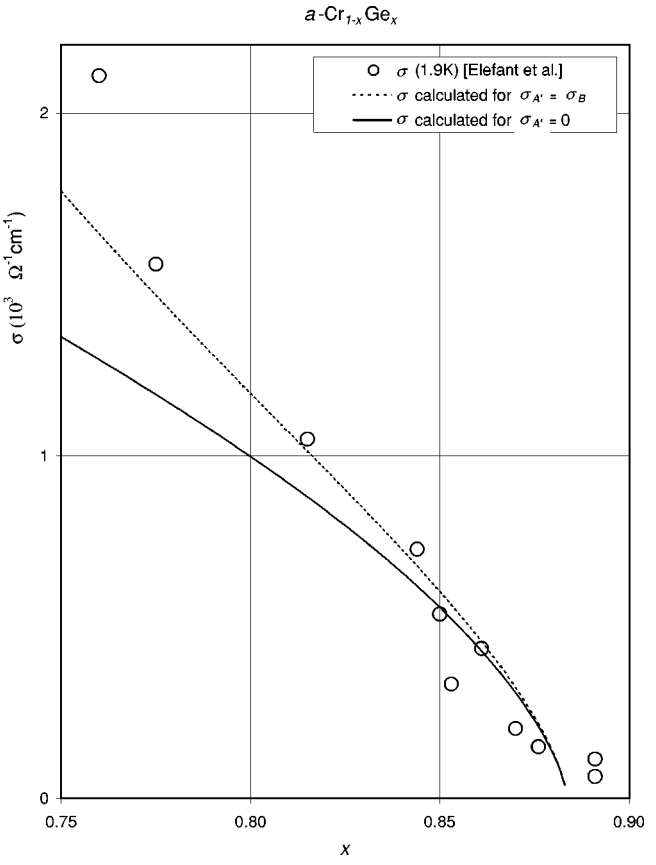

FIG. 7. Same as Fig. 5, but for a-$Cr_{1-x}Ge_x$ and comparison of the calculated $\sigma(x)$ dependence with experimental data taken from Elefant *et al.* (Ref. 87) (electron-beam evaporation).

The experimental conductivity data close to the M-I transition taken from Möbius[15] are described relatively well by the applied equations, and the enormous difference of the experimental σ data compared with those of Okuma *et al.*[9] can be caused by the different deposition conditions which had led to different phase grain sizes: While the samples of Möbius[15] were realized by evaporation from a Cr-Si *alloy* ingot, those of Okuma *et al.*[9] were realized by codeposition from *two separated sources*, a Cr source and a Si one, where concentration gradients about the samples cannot be completely avoided and, consequently, the M-I transition is expected to be "smeared out" over a finite concentration *interval* characterized by the fact that near x_c part of the B phase is still *metallic*, whereas another part is already insulating and that the *metallic* fraction of the B phase decreases as x increases.

Nevertheless, the relatively good agreement between the calculated and experimental $\sigma(x)$ dependence for the Möbius[15] data, as shown in Fig. 6, is surprizing considering the fact that each experimental data point represents another sample of an amorphous alloy for which both small variations in the deposition conditions (substrate temperature, deposition rate, vacuum, …) and uncertainties of the precise composition of the alloy, x, are to be considered. Moreover, the calculations are approximations, where (1) the phase grains were approximated as spheres, (2) $p_{\mathrm{loc}} \ll p$, and (3) $L_B/d_B \simeq 1$ was set. The approximation (1) leads to *smaller* values for p (and σ) in comparison to *nonspheric B* phase grains, for which v_{B^*}/v_B is larger than given by Eq. (2), whereas the approximation (2) leads to larger values for p (and σ) and is assumed to play a role only for very small p. The approximation (3) is assumed to be the worse the larger p considering the fact that the mean free path increases with the energy of the carriers[84–86] leading to the fact that the calculated $\sigma(x)$ curve lies below the experimental σ data, and this difference is expected to increase with increasing p (or σ). Another uncertainty comes from the assumption that the average phase grain size is independent of x.

From Fig. 6 it can be seen that the concentration, where the M-I transition, x_c, occurs, depends also on the average metal grain size, D_A: The larger D_A the smaller x_c, if the other physical parameters are constant.

a-$Cr_{1-x}Ge_x$ alloys

Finally, the calculated $\sigma(x)$ dependence for a-$Cr_{1-x}Ge_x$ is shown in Fig. 7 in comparison with experimental data taken from Elefant *et al.*[87] which are produced by electron-beam evaporation from ingots of Cr-Ge alloys. The physical parameters applied for the calculations were $\mathcal{N}_A = 7.9 \times 10^{22}\,\mathrm{cm}^{-3}$, $\mathcal{N}_B = 5.0 \times 10^{22}\,\mathrm{cm}^{-3}$, $d_B = 0.244$ nm, $\beta_v = 0.5$, $L_B/d_B \simeq 1$, $x_A = 0.25$, $x_B = 0.90$, $Z_{\mathrm{Cr}} = 0.5$, $Z_{\mathrm{Si}} = 4$, $D_A = 1.4$ nm,

and $p_{loc} \ll p$. From Eqs. (6), (19), and (20) it follows $\upsilon_{B,k} = 0.86$ corresponding to an atomic concentration of $x_k = 0.77$, and from the calculated $\sigma(x)$ curves in Fig. 7, $\upsilon_{B,c} = 0.98$ corresponding to $x_c = 0.88$, respectively. As can be seen, the calculated $\sigma(x)$ dependence describes relatively well the experimental data with the exception of the data point at the largest metal content ($x = 0.76$). Regarding the two data points at $x = 0.891$ we have to consider that the measuring temperature was $T = 1.9$K and that the $\lg(\sigma) - T^{-1/2}$ plots shown by Elefant *et al.*[87] (Figs. 1 and 2 in Ref. 87) have a negative temperature coefficient, and it seems to be not sure whether these samples are still metallic ($\sigma > 0$ at $T = 0$) or already insulating ($\sigma = 0$ at $T = 0$).

From Eqs. (5), (19), and (20) it follows that $\upsilon_A < 1/3$ is actually fulfilled in the whole concentration ranges considered in Figs. 5–7, i.e., the electronic transport in the *A* phase takes place by tunneling as assumed above (Sec. III A).

The calculations for the amorphous alloys shown in Figs. 5–7 are to be considered as example calculations. The precision of these calculations can be improved, when supplementary to the $\sigma(x)$ data experimental data for the physical parameters x_A, x_B, D_A, and $\mathcal{N}_A$, $\mathcal{N}_B$ are available, e.g., determined according to the examples of Refs. 31, 32 and 43, respectively. An additional test of the physical model presented can be realized by including measurements of the Seebeck and Hall coefficients in dependence on concentration, which provides the possibility for determination of the electron transfer between the phases and checking Eq. (1).

D. $S_{1-x}M_x$ alloys

In the phase separated range of $S_{1-x}M_x$ alloys, for calculation of the hole density in the *B* phase, *p*, the equations of Sec. III B can be applied, when Z_N in Eqs. (16) and (18) is replaced by Z_S, the valence of the *S*-atoms,

$$n_B = \mathcal{N}_B[(1 - x_B)Z_S + x_B Z_M], \tag{25}$$

$$n_A = \mathcal{N}_A[(1 - x_A)Z_S + x_A Z_M], \tag{26}$$

and Eq. (21) is replaced by

$$p_0 = 4\mathcal{N}_B\left(1 - \frac{\nu}{4}\frac{X_{B^*}}{X_B}\right). \tag{27}$$

ν is the number of free sp^3 orbitals per B^* atom which are not available for the VB caused by the fact that the atoms in the *A* phase (bordering on the B^* atoms) do not have sp^3 configuration. In analogy to the Davis-Mott model[56] these free sp^3 orbitals (of the B^* atoms) are assumed to provide a band of localized states in the energy gap of the *B* phase with the density of states

$$p_{loc1} = 2\nu\mathcal{N}_B\frac{X_{B^*}}{X_B}, \tag{28}$$

which adds to $2p_{loc}$ arising from dangling bonds and other structure defects between touching *B* phase grains and within the cores of the *B* phase grains (B_0). In Fig. 8 the calculated carrier densities, *n* and *p*, are shown for $Al_{1-x}Ge_x$ alloys. In the *two*-phase-range $x_A < x < x_B$, *n* and *p* are calculated with Eqs. (1)[82] and Eq. (14) in connection with Eqs. (15), (17), (19), (20), (22), and (25)–(27), where $\upsilon_{B^*}/\upsilon_B$ is calculated by Eqs. (2) and (7) for $\upsilon_B < 1/3$ and $\upsilon_B > \upsilon_{B,k}$, respectively, and linearly interpolated (relating to x_B) in the concentration range $1/3 < \upsilon_B < \upsilon_{B,k}$ with $\upsilon_{B,k}$ followed from Eq. (6). For the physical parameters the following values are applied: $\mathcal{N}_A = 6.0 \times 10^{22}\,\mathrm{cm}^{-3}$, $\mathcal{N}_B = 5.0 \times 10^{22}\,\mathrm{cm}^{-3}$, $d_B = 0.244$ nm, $\beta_\upsilon = 1.3$,[27] $D_A \simeq D_B \simeq 5$ nm, $x_A = 0.05$, $x_B = 0.56$, $Z_S = 3$, $Z_M = 4$, $p_{loc} = 0$, and $\nu = 1$. The value for x_B in the two-phase range is determined from the free enthalpy diagram for Al-Ge by Köster[88] (tangent construction). The value for β_υ was estimated from $\sigma(x)$ data measured at $T = 5$ K published by McLachlan *et al.*[70] applying EMT and Eqs. (11) and (32) under the assumption of $L_A \simeq D_A$ [crystalline Al(Ge) grains] and consideration of tunneling contribution through the *B* phase (to be studied in a separate paper).[89] In the *one*-phase ranges the carrier densities are calculated applying

$$n = \mathcal{N}_A[(1 - x)Z_S + xZ_M] \tag{29}$$

for $x \leqslant x_A$ and

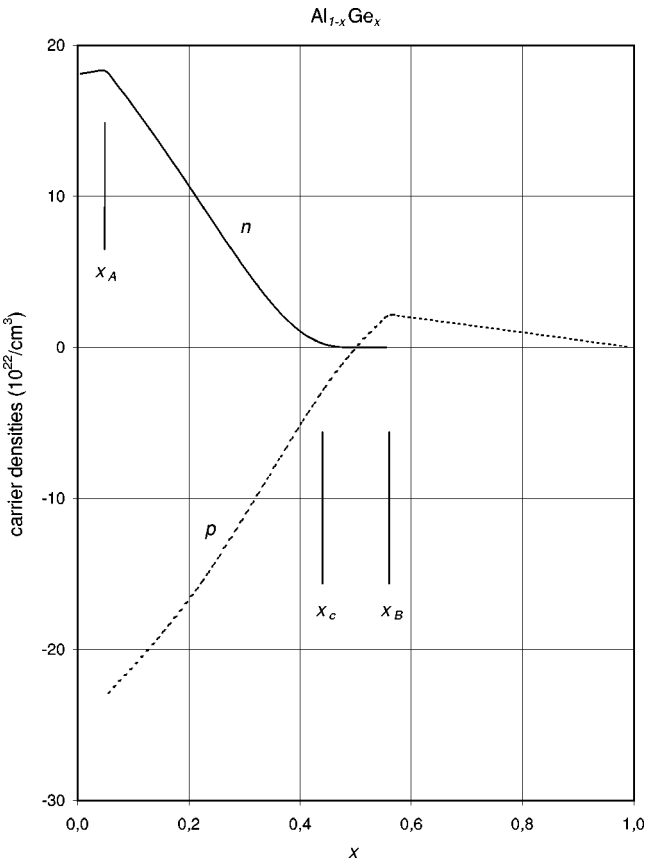

FIG. 8. Calculated carrier densities for $Al_{1-x}Ge_x$ applying Eq. (14) in connection with Eqs. (15), (17), (19), (20), (22), and (25)–(27) (*two*-phase range $x_A < x < x_B$) and Eqs. (29) and (30) (*one*-phase ranges $x \leqslant x_A$ and $x \geqslant x_B$, respectively), where $p_{loc} = 0$ and $\nu = 1$ was set: For $x_A < x \leqslant 0.5$, $p < 0$, i.e., the VB is completely filled and excess electrons occupy surface states on the phase boundaries. Consideration of $p_{loc} > 0$ shifts the $p(x)$ curve in direction to smaller values.

$$p = \mathcal{N}_B[4 - (1-x)Z_S + xZ_M] - p_{\mathrm{loc}} \tag{30}$$

for $x \geqslant x_B$. x_c, the concentration of the M-I transition, stated by McLachlan *et al.*,[70] and the assumed values for x_A and x_B are also drawn in Fig. 8. Since we are interested in the basical tendency, $p_{\mathrm{loc}}=0$ is set for the calculation of $p(x)$ in Fig. 8.

As can be seen in Fig. 8, two principle problems arise.

(a) The calculated hole density, p, results to be negative for $x \lesssim 0.5$, since the amount of transferred electrons described by Eq. (1) is larger than the number of electronic states available in the VB for x essentially smaller than x_B. The amount of p increases with decreasing x.

(b) For $x > x_c$, but x near to x_B, the $Al_{1-x}Ge_x$ alloys are electrically insulating, although p is essentially larger than zero.

Problems (a) and (b) also continue, if the assumed values for D_A, D_B, x_A, x_B, ν, and β_v are changed within the scope of physically reasonable values. The second problem, (b), can be asigned to the neglection of p_{loc}, since a nonzero p_{loc} shifts the p curve in direction to smaller p values. However, if so, then there is not yet an answer on the first problem, (a). Reason is the assumption made until now, that *both* the A and B phase grains are spherical. This assumption is apparently not true, generally, for *S-M* alloys. This fact corresponds with the *granular* structure[69,70,72,73,90] found experimentally for Al-Ge films on the metallic side, where nearly spherical grains are only formed by the metallic phase (phase A), whereas the phase B forms very thin Ge(Al) mantle surrounding the metallic grains (*modified physical model*) leading to a very increased boundary face regarding the B phase providing additional electronic states for acceptance of electrons transferred from the A phase. For such a microscopic structure the sum of all the boundary faces between the two different phases is considerably increased in comparison to a structure with *spherical* phase grains for *both* the phase A and phase B. In other words, the electron redistribution between the two phases affects the microscopic structure of the alloy as well.

Considering a single (spherical) A phase grain with the diameter D_A completely enveloped by a B phase coating which has the (constante) thickness δ_B, then it follows for $\delta_B \ll D_A$:

$$D_A = \frac{2\delta_B}{(\upsilon_{B^*}/\upsilon_A + 1)^{1/3} - 1}. \tag{31}$$

If $\delta_B = d_B$ (i.e., the B phase barrieres between two "touching" A phase grains has a thickness of *two* atomic monolayers), $X_{B0} = \upsilon_{B0} = 0$, and with Eqs. (4), (5), and (31) we get

$$D_A = \frac{2d_B}{\upsilon_A^{-1/3} - 1}. \tag{32}$$

In Fig. 9 the dependence of D_A on x described by Eq. (32) is drawn, where υ_A is replaced by

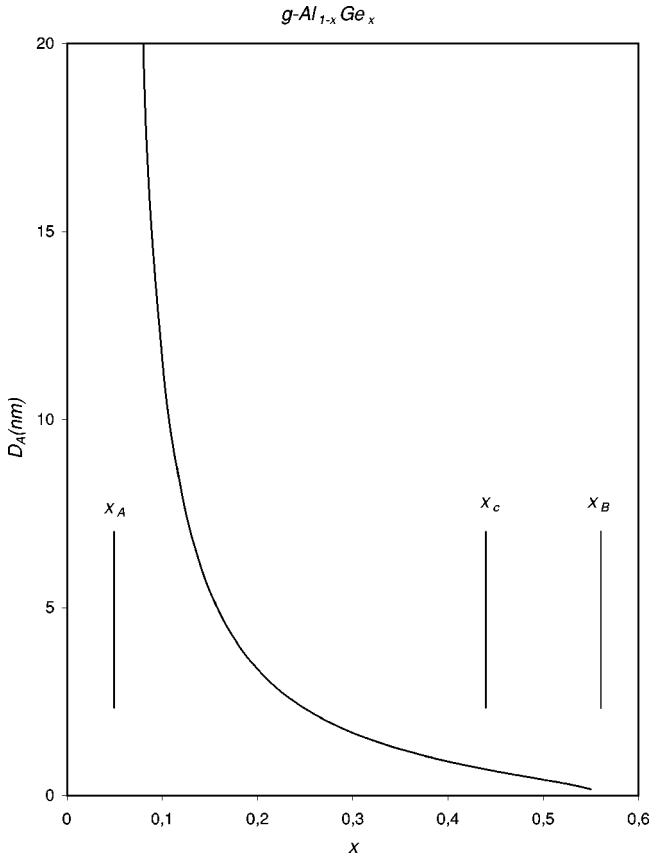

FIG. 9. Dependence of the average phase grain size, D_A, on x for g-$Al_{1-x}Ge_x$ calculated by Eqs. (32) and (33) for the *modified physical model*, where thin Ge(Al) mantle with the thickness of $2d_B$ is surrounding the spherical *metallic* Al(Ge) grains.

$$\upsilon_A = \left[1 + \frac{\mathcal{N}_A}{\mathcal{N}_B}\frac{(x - x_A)}{(x_B - x)}\right]^{-1}. \tag{33}$$

The concentration dependencies of both "$p(x)$" and $D_A(x)$ drawn in Figs. 8 and 9, respectively, are very well reflected by experimental results of as-deposited $Al_{1-x}Ge_x$ films published by Lereah *et al.*,[73] McLachlan *et al.*,[70] Rosenbaum *et al.*,[42] and Catalina and Afonso.[72]

(1) On the insulating side ($x > x_c$), both the Ge and the Al components (phases) are found to have amorphous structure. This finding corresponds with Fig. 8: *charged* phase grain faces (prerequisite for *granular* structure) are not yet or hardly formed, because $|p|$ is small. On the metallic side ($x < x_c$), *granular* Al grains embedded in an amorphous matrix are found: reason are the *charged* phase boundary faces, because $p < 0$ and $|p|$ is large, Fig. 8.

(2) On the insulating side ($x > x_c$), the (*amorphous*) Al grains are found to be smaller than <2 nm, whereas, on the metallic side ($x < x_c$), the (*granular*) Al grains rapidly increase to 10–20 nm, in correspondence with the semiquantitative consideration, Fig. 9.

(3) The M-I transition takes place at relatively large metal content ($x_c = 0.56$). The reason is the fact that the VB does not contribute to the electronic transport, since completely occupied (at $T=0$) and, as a consequence, the M-I

transition takes place, if the *A* phase does no longer form an infinite cluster through the specimen. With increasing x (or υ_B), the probability for interruption of the infinite *A* phase cluster increases, and for the special laminared *B* phase structure this interruption is expected to occur at relatively small x (or υ_B). We assume that, for small x, the *B* phase covers do not *completely* cover the *A* phase grains, but that there are *A*-*A* phase grain contacts, which are the prerequisite for an infinite *A* phase cluster.[91] If an infinite *A* phase cluster does no longer exist, tunneling of electrons through the *B* phase films does not lead to a metallic conductivity (characterized by $\sigma>0$ at $T=0$) because of the charging energy to be overcome between different *A* phase grains. The situation is comparable with those in cermets described by Abeles *et al.*[77–79]

Within the *modified physical model* the density of states in the laminared *B* phase results for $\delta_B=d_B$:

$$p_0 = 4\mathcal{N}_B\left(1-\frac{\nu}{4}\right) \tag{34}$$

and

$$p_{\mathrm{loc1}} = 2\nu\mathcal{N}_B \tag{35}$$

following from Eqs. (27) and (28), respectively, for $X_{B0}=\upsilon_{B0}=0$. In sum, for all the electrons in the *B* phase, the own electron density, n_B, Eq. (25), and the transferred one, Δn, Eq. (17), there are below the conduction band of Ge(Al)

$$p_0 + p_{\mathrm{loc1}} = 4\mathcal{N}_B\left(1+\frac{\nu}{4}\right) \tag{36}$$

electronic states per volume unit, which for $\nu=1$ is $\simeq 25\times10^{22}\ \mathrm{cm}^{-3}$, and comparing with Fig. 8, in the concentration range $x>x_A$, $p_0+p_{\mathrm{loc1}}>n_B+\Delta n$, generally. Only for very small x (but $x>x_A$), p_0+p_{loc1} is nearly comparable with $n_B+\Delta n$ corresponding to an average number of $\simeq 5$ electrons per B^* atom. This estimation is to be considered as temporary, as it depends sensibly on the value for β_υ applied.[89] Replacing Eq. (27) by Eq. (34), $p<0$ for the complete *two*-phase range, i.e., metallic conductivity in the VB ($\sigma_B>0$ for $T=0$) is not expected for $x_A<x<x_B$ [problem (b) mentioned earlier]. And in the *one*-phase range $x\geqslant x_B$, metallic conductivity does also not occur because of $-p_{\mathrm{loc}}$ (arising from dangling bonds and other structure defects) (Ref. 92) shifting the $p(x)$ curve into direction of negative values.

Summarizing, the experimental findings, granular structure for large metal content, but amorphous structure for small metal contant, rapid decrease of the average metal grain sizes with increasing x (or υ_B), and relatively small x_c, follow informely from the *modified physical model* described.

The *modified physical model* can also be basis for a model of the class of cermets[77,79] for which both the *granular* structure and decrease of the metal grain size with decreasing metal content are characteristic features (see, e.g., Abeles *et al.*,[77] Figs. 13–16, 17, and 19 therein).

Comparing $S_{1-x}M_x$ alloys with $N_{1-x}M_x$ alloys, a crucial difference consists in the fact that in the latter each B^* atom in the $M(N)$ phase (*B* phase) provides eight electronic states to the VB (2 *s*, 3 *bonding p* states, and 3 *antibonding p* states), whereas in the case of $S_{1-x}M_x$ alloys each B^* atom provides only $4\text{-}\nu$ electronic states to the VB. Another difference is the fact that in $N_{1-x}M_x$ alloys, there are *d*-*p* bondings at the interfaces between the different phases, whereas in $S_{1-x}M_x$ alloys *d*-*p* bondings are absent, i.e., bonding between the different next-neighbored phase ranges (*A* and *B*) in $S_{1-x}M_x$ alloys is essentially determined by *Coulomb attraction*, whereas in $N_{1-x}M_x$ alloys *band structure* energy arising from the *d*-*p* bondings plays an additional role.

Regarding the incompletely occupied VB, in $a\text{-}T_{1-x}M_x$ alloys the situation is expected to be comparable with those in $a\text{-}N_{1-x}M_x$ alloys, however, with the difference that the M-I transition can take place between other phases (Sec. II A) than in $a\text{-}N_{1-x}M_x$ alloys. In $c\text{-}N_{1-x}M_x$ and $c\text{-}T_{1-x}M_x$ alloys the situation is, on principle, expected to be comparable with those in $a\text{-}N_{1-x}M_x$ and $a\text{-}T_{1-x}M_x$ alloys, however with the differences described in Sec. II A.

Although in *random* $S_{1-x}M_x$ alloys ($r\text{-}S_{1-x}M_x$) the M-I transition occurs at relatively large metalloid content, an incompletely occupied VB is, nevertheless, inprobable in these alloys; reason for such large x_c (or $\upsilon_{B,c}$) is suggested to be caused by the clefted "fjord"-like or "fractal" structure[73] realizing a possiblest large surface of the phase boundary for acceptance of all the transferred electrons for which in the VB there are not a sufficient number of electronic states. Typical for such a "fractal" structure in *r*-Al-Ge are "Al-Ge colonies" (Lereah *et al.*[73]) where Ge crystals with a dense branching morphology are completely surrounded by a rim of Al-rich single-crystal matrix which acts as *large metallic* grains, although each of these *large metallic* grains contain a considerable volume fraction of the *non metallic* phase. Such a "fjord"-like or "fractal" structure growing by annealing of $g\text{-}S_{1-x}M_x$ alloys, has been intensively studied by Lereah *et al.*,[73] see, e.g., Figs. 1 and 6 of Ref. 73.

IV. DISCUSSION

A. EMT

The EMT and their results are often considered to be suspect,[77,93] especially for description of the M-I transition for which the EMT and percolation theory provide different volume fractions of the *metallic* component embedded in an *insulting* matrix: "0.15" following for the percolation threshold[94] determined by a Monte Carlo sampling of disordered three-dimensional resistor networks and "1/3" following from the EMT, Eq. (8). This difference between the percolation theory and the EMT was in the past one reason for a reservation against the EMT which is considered to be "unreliable in the transition region $C\leqslant 0.4$ and below" (Ref. 93, C corresponds to our υ_A), and consequently also for describing the M-I transition. A second reason for this reservation against the EMT were considerable differences between the predictions by the EMT and the experimental results to both the concentration dependence of the conductivity, $\sigma(x)$, and the concentration of the M-I transition, x_c, in cermets (see, e.g., Ref. 77, Fig. 19 therein).

In spite of this reservation, we expect that the EMT provides for metal-metalloid alloys a more realistic description

for the transport properties (also near to the M-I transition) than the percolation theory because of the following reasons.

(1) In real disordered alloys the occupation of the "sites" by the *A* and *B* phase grains does not occur completely *accidentally* or *randomly*: in the next neighborhood of an *A* phase grain the probability for finding of *B* phase grains is larger than it would be, when the *A* and *B* phase grains would be completely *accidentally* distributed in the alloy as assumed in the percolation theory. The reason is the fact that in the two-phase region the average composition of the surrounding of this *A* phase grain tends away from the average composition of the alloy into the direction of the *B* phase composition. Vice versa, in the surrounding of a *B* phase grain the composition tends rather into the direction of the *A* phase composition. Therefore, the interrupt of an infinite cluster of connected *A* phase grains through the sample is shifted to a larger volume fraction of the metallic component in comparison to an completely *accidental* arrangement of the phase grains. From this point of view, the EMT prediction for the interrupt of an infinite *A* phase cluster at $v_A = 1/3$ seems to be rather probable than the percolation theory prediction, $v_A = 0.15$.

(2) Regarding granular metals or cermets, the considerable differences between experiment and the EMT predictions quoted earlier[77] can often be caused by the simple assumption made that $x = X_B$ which is not true in many cases, since the insulating component can contains a considerable fraction of metal atoms,[95] and also the metallic component can contain a considerable fraction of metalloid atoms. Regarding a-$N_{1-x}M_x$ or a-$T_{1-x}M_x$ alloys we recall at the result of Sec. III that the M-I transition must not be determined by interrupt of a "metallic" phase, because in the phase separated range, the phase *a*-Si or *a*-Ge can be *metallic* as well depending on the amount of the electronic states arising from the internal surfaces (B^*) and their occupation by electrons leading to the fact that the M-I transition in these systems occurs at concentrations essentially different from $x = 1/3$ (or more precise $v_A = 1/3$). Because of these reasons, we assume that the EMT provides a more realistic description of the electrical properties of disordered alloys with phase separation than any percolation description.

B. BTE and NFE approximation

Today, there is a general consensus that:

(a) *NFE approximation* is not an appropriate method for description of the electrons in strongly scattering systems as, e.g., metal-metalloid alloys. This point of view has been hardened after in the past "the great majority of experimental papers have attempted to explain the data by an uncritical application of nearly free electron (NFE) ideas" (Howson and Gallagher).[96] The same point of view has been also consolidated regarding the

(b) *BTE: when the mean free path of the carriers, L, becomes comparable with the average atomic distance, d, the wave number k is no longer a good quantum number for describing the eigenstates and the BTE cannot be applied.*[16,17]

Now we shall show that consideration of *phase separation* in disordered metallic alloys can lead to an alternative point of view. We give two arguments, a theoretical argument and an experimental example.

Historically seen, view (b) cited earlier was concluded from the fact that in metals[97]

$$k_F \simeq \frac{\pi}{d}, \tag{37}$$

where k_F is the wave number at the Fermi surface. Inserting Eq. (37) and measured σ data of any metal-metalloid alloy on the metallic side, but close to the M-I transition, in the BTE:

$$\sigma = \frac{S_F e^2 L}{6\pi^2 h}, \tag{38}$$

and assuming a spherical Fermi surface $S_F = 4\pi k_F^2$, then it follows $L < d$, which is physically not possible, because the average free path cannot be smaller than the average distance of the scattering centers. However, considering phase separation, with decreasing fraction of the "metallic" phase (in the two-phase range), Eq. (37) is no longer valid and Eq. (38) is to be applied to the two phases separately, where each phase has its "own" Fermi surface, if $v_A > 1/3$, $v_B > 1/3$ (Sec. III A). And the carrier densities in the two phases are essentially different from a situation corresponding to Eq. (37).

Since the electron density in the metallic phase decreases with increasing x (or with increasing ζ), k_F in the phase *A* decreases as well according to

$$k_F = (3\pi^2 n)^{1/3} \tag{39}$$

(spherical Fermi surface and NFE approximation). For the hole density p in the phase *B*, the situation is analoguous, because p decreases with increasing x as well (*N-M*, *T-M* alloys, see Secs. II and III). This leads to the fact that application of the BTE in NFE approximation and $\sigma(x)$ data for any metallic alloy remains compatible with the condition "$L \geqslant d$" even near the M-I transition.

Experimental example: Mizutani and Yoshida[98] have shown for a-$(AgCu)_{1-x}Ge_x$ alloys that for $x < 0.3$ there is a good agreement between the measured Hall coefficient data, R_H, and the free-electron values

$$R_{H0} = (en_0)^{-1} \tag{40}$$

derived from the BTE in NFE approximation, where n_0 is the total valence electron density in the alloy [Eq. (8) of Pap. I] This agreement between R_H and R_{H0} gives the justification for application of the BTE in NFE approximation to the *conductivity* for $x < 0.3$ as well. Applying Eq. (11) to the measured σ data[98] of a-$(AgCu)_{1-x}Ge_x$ for $x < 0.3$, where $\sigma_A = \sigma$ (one-phase range), it follows that $L \simeq d$ for $0.2 < x < 0.3$.[74] In other words, in the concentration range $0.2 < x < 0.3$ the BTE in NFE approximation provides a good description for the Hall coefficient, although $L \simeq d$ is already reached. This is in contradiction to the view that k_F is no longer a good quantum number, since L is comparable with d.

With these two arguments, and in agreement with the alternative concept of Pap. I, we propose an *alternative inter-*

pretation: *L cannot be smaller than d*; *therefore in disordered electronic systems, d is the lower limit for L, and k can be considered as a good quantum number for describing the eigenstates, as long as*

$$kL > c^*, \tag{41}$$

where c^* is of the order of 1 (Ref. 99) (Ioffe-Regel criterion). The decisive difference to the point of view (b) cited earlier is the fact that (independent of the degree of disorder represented by the mean free path L) the electronic states can be extended for connected ranges of the same phase, and the concept of a Fermi surface is after all applicable, as long as Eq. (41) is fulfilled, even for $L \simeq d$. Considering the experimental example a-$(AgCu)_{1-x}Ge_x$, the abrupt splitting between n_0 and $n_H=(eR_H)^{-1}$ at $x \simeq 0.3$ is a consequence[74] of the beginning phase separation for $x \gtrsim 0.3$, because only still part of the total electron density is available in the phase A due to the electron redistribution to the second phase [Eq. (1)]. On the other hand, in *granular* metal-metalloid alloys (Sec. III D) on the metallic side the Fermi level lies in ranges of trap states in the phase B, however, in ranges of extended states in the phase A.

For consideration of the electronic transport processes in a phase at $T=0$ we concentrate our attention to k_F:

$$k_F > \frac{c^*}{L}. \tag{42}$$

For the case when scattering is strong, L can approach d, but cannot be smaller than d, and with Eq. (42) it follows a lower limit, where k_F still can be applied for description of the wave functions of the carriers at the Fermi surface, given by

$$k_F \gtrsim \frac{c^*}{d}, \tag{43}$$

if $L \simeq d$ is realized. k_F in Eqs. (42) and (43) is limited to *continuous* range of atoms with overlapping wave functions. Outside of this range the wave functions decrease exponentially. Now let us consider the question of whether and under which conditions the BTE and NFE approximation can be applied for disordered alloys with phase separation. The decrease of n with increasing x or ζ [Eq. (1)] leads also to decrease of the Fermi energy, E_F, in the phase A, and the corresponding Fermi surface approaches a spherical form also in *crystalline* alloys, the smaller n, approaching a NFE behavior, since the Fermi surface for phase A is sufficiently distant to the first Brillouin zone boundary, when n is sufficiently small. The situation in phase B is similar regarding the hole density p for sufficiently large v_B, where p is small (see Secs. II and III). This is especially so near to the M-I transition, provided Eq. (42) is still fulfilled.

C. Minimum metallic conductivity

Because of Eq. (42)—in connection with Eq. (39)—there exists a lower limit for n, below it extended electronic states cannot be exist. Regarding Eq. (42), in the literature different values[99] for c^* are given ranging from $1/2\pi$ until π which differ by a factor of 20 corresponding to a factor of 4 orders of magnitude for n according to Eq. (39), and because of this large span for n the question of the lowest possibly limit of $k_F L$ becomes importantly. From Heisenberg's uncertainty principle it follows $c^*=1/4$ (see the Appendix) and we define this value as the lowest possibly limit where extended electronic states still can exist. When n decreases below n_{crit} given by

$$n_{\mathrm{crit}} = \frac{1}{3\pi^2}\left(\frac{c^*}{L}\right)^3, \tag{44}$$

corresponding to a minimum metallic conductivity

$$\sigma_{\min} \simeq \frac{c^*}{6}\left(\frac{e^2}{h}\right)\frac{1}{L}, \tag{45}$$

latest then localization in the metallic phase of a disordered alloy must occur. Equations (44) and (45) result from Eqs. (11), (39), and (42). For strong scattering characterized by $L \simeq d \simeq 0.25$ nm it follows from Eqs. (44) and (45):

$$n_{\mathrm{crit}} \simeq 3 \times 10^{19}\ \mathrm{cm}^{-3} \tag{46}$$

and

$$\sigma_{\min} \simeq \frac{c^*}{6}\left(\frac{e^2}{h}\right)\frac{1}{d} \simeq 20\ \Omega^{-1}\,\mathrm{cm}^{-1}. \tag{47}$$

For a nearly completely filled band the same equations, Eqs. (41), (43), (45), and (47), hold, where L has the meaning of the mean free path of the holes at the Fermi energy of the nearly completely filled band, and for the critical hole density it follows:

$$p_{\mathrm{crit}} = \frac{1}{3\pi^2}\left(\frac{c^*}{L}\right)^3, \tag{48}$$

which for strong scattering, i.e., $L \simeq d \simeq 0.25$ nm, again leads to

$$p_{\mathrm{crit}} \simeq 3 \times 10^{19}\ \mathrm{cm}^{-3}. \tag{49}$$

The first equation of Eq. (47) looks like the original relation for a minimum metallic conductivity derived by Mott with $c^*/6 \simeq 0.026 \cdot 2\pi$ (Ref. 16, p. 30), where additionally the disorder effect by *random* potentials was considered. The difference consists in the fact that for the derivation of Eqs. (44), (45), and (48) *random* atomic potentials within a single phase are not assumed. In other words, we cannot see any reason for the assumption that in one of the two phases of an alloy with phase separation there would be essential potential fluctuations *growing* with increasing v_B from $v_B=0$ to larger values until $v_{B,c}$ (the B phase fraction at the M-I transition) or beyond it. The disorder effect on the electronic transport properties can be characterized alone by the "ordering parameter" L, and, if $L \simeq d$ is already realized, σ at $T=0$ decreases (with increasing v_B) not by further increasing "disorder," but by decrease of n or/and p according to the formulae of Secs. II and III.

The conclusion of a minimum metallic conductivity $\sigma_{\min}$ seems to be in contradiction to the conclusion by Okuma *et al.*[9] and Hertel *et al.*,[8] that the M-I transition in a-$Cr_{1-x}Si_x$ and a-$Nb_{1-x}Si_x$ occurs continuously and that for $T \to 0$, es-

sentially smaller σ were measured than 20 $\Omega^{-1}\mathrm{cm}^{-1}$. This finding is, however, not really in contradiction considering the fact that the samples are produced by coevaporation[9] and cosputterring[8,9] from two locally *separated* sources, one with the element Cr or Nb and the other with the element Si, and in the samples a concentration gradient is to be expected. If there is a concentration gradient perpendicularly to the direction of the measuring current for measurement of σ, then a *continuous* M-I transition with increasing (average) x can be pretended, because the sample occurs to be *metallic* as long as there is still a narrow *metallic* current path through the sample. A concentration gradient is connected with a gradient of ζ and leads, therefore, also to a gradient of p (according to the equations of Secs. II and III). Immediately at the M-I transition locally limited *metallic* ranges ($p>p_{\mathrm{crit}}$, $\sigma>0$ at $T=0$) and locally limited *insulating* ranges ($p<p_{\mathrm{crit}}$, $\sigma=0$ at $T=0$) can coexist leading to an *average* $\sigma<\sigma_{\mathrm{min}}$ at $T=0$, i.e., the M-I transition can be smeared out across a concentration *range* and the resulting conductivity at $T=0$ can be smaller than given by Eqs. (45) and (47) caused by the "dilution" of the *metallic* fraction within a phase. As long as there is still a connected cluster of *metallic* ranges (of the same phase) through the whole sample, this sample shows *metallic* conductivity ($\sigma>0$ at $T=0$). Moreover, we have to take into account that L can be larger than d (for instance in *crystalline* alloys) corresponding to a smaller σ_{min} according to Eq. (45) compared with Eq. (47).

Möbius *et al.* concluded from phenomenological considerations of conductivity data of a-$Ni_{1-x}Si_x$ (Ref. 10) and a-$Cr_{1-x}Si_x$ (Refs. 11–15) that the M-I transition is very likely discontinuous at $T=0$. This conclusion corresponds with our result of a minimum metallic conductivity in a metallic phase.

D. Mobility edges and comparison with photoelectron spectra

For a nearly empty parabolic band in NFE approximation, the density of states is given by $N(E)=4\,mk/h^2$, and—replacing k by Eq. (41)—it follows for the density of states at the mobility edge, E_C:

$$N(E_C)=\frac{4c^{*}m}{h^2L}, \tag{50}$$

and for the energy at the mobility edge, E_C:

$$E_C=E_A+\frac{(c^{*}\hbar/L)^2}{2m}, \tag{51}$$

where m is the effective electron mass, E_A characterizes the bottom of the band.

For a nearly filled parabolic band in NFE approximation it follows for the density of states at the mobility edge, E_V:

$$N(E_V)=\frac{4c^{*}m}{h^2L}, \tag{52}$$

and for the energy at the mobility edge, E_V:

$$E_V=E_B-\frac{(c^{*}\hbar/L)^2}{2m}, \tag{53}$$

where m and L have the meaning of an effective mass and mean free path of the holes at the Fermi energy of the nearly filled band. E_B characterizes the top of the band.

For the case of strong scattering, in Eqs. (50)–(53), L is to be replaced by d. For any (nonparabolic) band, Eqs. (51) and (53) no longer have a physical meaning in this context and we apply the terms E_C and E_V only to characterize the points on the energy scale, where $N(E)$ crosses a mobility edge defined by Eqs. (50) and (52). In other words, Eqs. (50) and (52) can be applied to define mobility edges also for any (nonparabolic) band, provided effective masses can be defined according to

$$\frac{1}{m}=\frac{1}{\hbar^2}\frac{\partial^2 E}{\partial k^2} \tag{54}$$

with a defined $E(k)$ dependence for $kL>c^{*}$, Eq. (41), in accordance with the *alternative interpretation* proposed in Sec. IV B.

Applying the discussion of Sec. III, the M-I transition in an a-$N_{1-x}M_x$ or a-$T_{1-x}M_x$ alloy takes place, when p decreases below p_{crit}, Eqs. (48) and (49), provided $v_{A,c}<1/3$, or, within the density of states picture: When the Fermi level μ lies beyond E_V, then the corresponding *metallic* conductivity in the phase disappears, $\sigma=0$ at $T=0$. The finding of a finite electronic specific heat coefficient γ beyond the M-I transition in a-$Mo_{1-x}Ge_x$,[33,34] a-$Au_{1-x}Si_x$,[35] a-$V_{1-x}Si_x$,[36] and a-$Ti_{1-x}Si_x$ (Ref. 37) quoted in Sec. I, can be caused by the *finite* hole density p in the VB [$0<p<p_{\mathrm{crit}}$ corresponding to $0<N(\mu)<N(E_V)$, $v_B>v_{B,c}$; $N(\mu)$ is the density of states at μ]. In the case of a-$V_{1-x}Si_x$, Mizutani *et al.*[36] found also from x-ray photoelectron spectroscopy (XPS) valence band spectra, "that the density of states at the Fermi level is definitely finite even in the insulating regime," although precipitation of V clusters is absent in the a-$V_{1-x}Si_x$ samples,[36] i.e., $\sigma=0$ at $T=0$, although the density of states at the Fermi level μ is finite, corresponding with our interpretation that for the insulating side $0<p<p_{crit}$ corresponding to $0<N(\mu)<N(E_V)$.

High-resolution photoemission (XPS and ultraviolet photoelectron spectroscopy) spectra profiles near the Fermi level for amorphous alloys[23,36,65,100–102] show a *band profile* around the Fermi edge μ, where above a critical metal content, $1-x_m$, $N(\mu)$ increases with increasing metal content, $1-x$:[103] a-$Ti_{1-x}Si_x$ (Kawade *et al.*,[23] Fig. 7 therein), a-$Pd_{1-x}Ge_x$ (Suzuki *et al.*,[101] Fig. 3 therein), a-$Ag_{1-x}Ge_x$ (Suzuki *et al.*,[65] Fig. 3 therein), a-$Ni_{1-x}Si_x$ (Isobe *et al.*,[100] Fig. 6 therein), a-$V_{1-x}Si_x$ (Mizutani *et al.*,[36] Fig. 14 therein), a-$Pd_{1-x}Si_x$ (Tanaka *et al.*,[102] Fig. 6 therein). This *band profile* near μ corresponds with our VB superimposed by the d states of the metal atoms forming bonds[60] with the p states of the M atoms. The increase of the hole density p with decreasing x (corresponding with the increase of σ in Figs. 5–7) corresponds with the increase of $N(\mu)$ in the *band profile*.

The values for $(1-x_m)$ resulting from the spectra are relatively small, where phase separation in the alloy is surely not yet realized: $1-x_m \approx 0.013$ for a-$Pd_{1-x}Ge_x$,[101] $1-x_m \approx 0.04$ for a-$Ti_{1-x}Si_x$,[23] $1-x_m \approx 0.056$ for a-$Ag_{1-x}Ge_x$,[65] $1-x_m \approx 0.07$ for a-$Ni_{1-x}Si_x$,[100] and a-$V_{1-x}Si_x$.[36] Only for a-$Pd_{1-x}Si_x$,[102] $1-x_m \approx 0.12$ is assumed to be in the two-phase region. The finding that $1-x_m$ lies in the one-phase region, is not in contradiction to our interpretation: in the one-phase region ($x > x_B$) the N or T atoms solved in the a-M-matrix provide electrons which occupy the band tail (arising from defect states) on the top of the valence band of a-M. With increasing metal content solved, the valence electron concentration decreases, since the N or T atoms do contribute essentially fewer electrons per atom to the VB than the host M atoms, i.e., the Fermi level moves into direction to larger density of states (within the upper valence band tail) corresponding to an increase of $N(\mu)$ with decreasing x. As long as $N(\mu) < N(E_V)$, $\sigma = 0$ at $T = 0$, i.e., the samples are insulating, although $N(\mu) > 0$. With beginning of the two-phase situation ($x \leqslant x_B$) the states with the s^2p^2 orbital configuration of the B^* atoms add to the valence band (now VB, phase separated region), and $N_B(\mu)$, the density of states in the B phase at $E = \mu$, increases. Note that the measured density of states is a superposition of the contributions of the two phases, $N_A(E)$ and $N_B(E)$, where near to x_c those of the B phase dominates. The M-I transition occurs, when μ crosses the mobility edge corresponding to $N(\mu) = N(E_V)$. The increase of $N(\mu)$ [or more precise $N_B(\mu)$] with decreasing x is reduced by the electron transfer *realizing* a *common* Fermi level μ for the whole sample.

In Eq. (14) the upper band tail of the VB (above E_V) is considered indirectly by the introduction of p_{loc} which is subtracted from the total hole density in the VB.

V. SUMMARY

The conclusions *amorphous phase separation* (i) and *band separation* (ii), where the carriers can be freely propagating and the corresponding wave functions are extended with respect to connected phase ranges, drawn in Pap.I for amorphous transition-metal-metalloid alloys, are now confirmed or supported by experimental and theoretical results by independent authors. *Conclusion* (iii), *electron redistribution (electron transfer) between the phases* [Eq. (1)] is not yet confirmed by independent authors.

Because of this confirmation and support of the *conclusions* (i) and (ii), the *amorphous phase separation model* developed in Pap. I, is extended to $N_{1-x}M_x$, $T_{1-x}M_x$, and $S_{1-x}M_x$ alloys: Phase separation in two phases with different SRO (i) leads to band separation (ii) in two electronic bands, the CB constrained to phase A, and the VB constrained to phase B. B is the phase with the deeper average potential. The electronic transport in the phase separated regime is determined by both the *local band structure* in the different phases and the *electron distribution* between the phases, where (1) the internal surfaces (phase boundaries), (2) the average compositions of the two phases, x_A and x_B, and (3) electron redistribution (electron transfer) between the phases plays a crucial role. An electron moving through the alloy is *not restricted to a single phase*, but it can overcome the phase boundaries, provided both the CB and the VB are incompletely occupied.

Considering valence band spectra it is assumed that for a-$N_{1-x}M_x$ and a-$T_{1-x}M_x$ alloys, in the two-phase range between a-Si or a-Ge (=phase B) and the next amorphous phase (=phase A), the VB consists essentially of bonding p and antibonding p states (from B atoms at the A/B boundary faces called B^* atoms) and of bonding sp^3 states (from *core* atoms of the B phase grains called B_0 atoms), Figs. 1 and 2, and for the VB generally hole conductivity is expected, because both a considerable part of the antibonding p states and the bonding sp^3 states are below the common Fermi level (chemical potential μ), whereas all the antibonding sp^3 states (of the B_0 atoms) are above the VB separated by an energy gap. The considerable fraction of antibonding p states below μ[60] supports the assumption of a considerable electron transfer from the A phase to the B phase and corresponds to the conclusion (iii) (Sec. I).

In $S_{1-x}M_x$ alloys the boundary faces between phase grains of the *different* phases are characterized by the transition from the tetrahedrally coordinated SRO with sp^3 hybrid orbitals [phase $B = M(S)$] to the close-packed structure typical for metallic phases with s^2p orbitals[57] [phase $A = S(M)$]. For those fractions of S atoms which are solved in the M matrix, the orbital configuration is assumed to be the sp^3 one; the hole density in the VB without considering electron transfer, p_0^*, is increased with the fraction of S atoms solved in the B phase, but decreases with increasing A/B phase boundary faces.

In the known metal-metalloid-alloys the M-I transition occurs apparently in the *two-phase* range, i.e., the M-I transition is suggested to occur by percolation of a metallic component. However, there are two essential differences to *classical* percolation theory:[94,104,105] (1) the "metallic" conductivity can be composed of two different conductivity contributions (arising from the two phases A and B), which additionally depend on concentration x. (2) The arrangement of the phase grains is not completely accidental as assumed by percolation theory. Therefore, for the phase separated ranges, the EMT is prefered for a quantitative description of the electronic conductivity σ, where to each of the two phases own transport coefficients are asigned, σ_i, α_i, $\kappa_{e,i}$, and $R_{H,i}$, for the phase i ($i = A, B$).

In *disordered*[106] $N_{1-x}M_x$ and $T_{1-x}M_x$ alloys, σ decreases with increasing x, as the carrier densities in both the CB and the VB, n and p, respectively, decrease as ζ increases.

In $N_{1-x}M_x$ alloys and in many $T_{1-x}M_x$ alloys the M-I transition is determined by the VB (phase B); however it takes place simultaneously (at the same concentration) in the A phase, if $v_{A,c} < 1/3$, since in this case electronic transport in the phase A takes place by tunneling.

In $S_{1-x}M_x$ alloys, the M-I transition is determined by the CB (phase A), since the states available in the VB are generally not sufficient for acceptance of all the electrons (enclosed the electrons transferred to the B phase) leading to charged phase boundaries. This fact is reason for (1) the *granular* structure, (2) the rapid decrease of the average phase grain size with increasing x, and (3) the relatively small x_c (or $v_{B,c}$) as well as for the *fractal* structure in

r-Al-Ge developing by annealing of *g*-Al-Ge.

From a critical discussion of the consequences of phase separation regarding the Ioffe-Regel criterion an *alternative interpretation* is proposed: the *mean free path, L, cannot be smaller than the mean atomic distance, d*; *therefore in disordered electronic systems, d is the lower limit for L, and k can be considered as a good quantum number for describing the eigenstates, as long as the Ioffe-Regel criterion* $kL > c^*$ *is not violated*. c^* is determined to be 1/4. This *alternative interpretation* provides the conditions for applicability of both the BTE and NFE approximation for disordered alloys with phase separation. The existence of a minimum metallic conductivity for a *homogeneous* electronic system or a metallic phase, $\sigma_{\min} \simeq (c^*/6)(e^2/h)(1/d) \simeq 20\,\Omega^{-1}\mathrm{cm}^{-1}$, is concluded for the case, that the scattering is strong characterized by $L \simeq d$, i.e., the M-I transition is concluded to be *discontinuous*. The seemingly contrary experimental finding of both metallic conductivities essentially smaller than 20 $\Omega^{-1}\mathrm{cm}^{-1}$ and continuous M-I transition in dependence on concentration can be pretended by local concentration fluctuations (e.g., by co-deposition from separated material sources). Smaller $\sigma_{\min}$ are also to be expected, if $L > d$ because of $\sigma_{\min} \simeq (c^*/6)(e^2/h)(1/L)$. The conclusion of a $\sigma_{\min}$ in the sense as described, involves also the existence of mobility edges which, as consequence of the alternative interpretation of the Ioffe-Regel criterion, can be described for a parabolic band in NFE approximation by Eqs. (50)–(53). For a nonparabolic band the mobility edges can be defined by the density of states, Eqs. (50) and (52), provided effective masses can be defined for $kL > c^*$.

Summarizing, Mott's original idea of a minimum metallic conductivity $\sigma_{\min}$ is supported by the alternative concept described.

The presented calculations are to be considered as example calculations and guide for new experiments which can improve the precision of the results, where experimental data as x_A, x_B, $\mathcal{N}_A$, $\mathcal{N}_B$, D_A, D_B, σ, α, and R_H versus x are useful. The necessary transport equations for α and R_H combining the EMT with the BTE, analogous to Eqs. (8)–(12) as well as tunneling of electrons for $\upsilon_A < 1/3$ and $\upsilon_B < 1/3$ will be subject of separated papers.

ACKNOWLEDGMENTS

The author would like to thank Professor Dr. Hellmut Keiter from the University of Dortmund and Dr. Martin Lange from the Katholieke Universiteit Leuven, for proofreading the manuscript of this paper. He also acknowledges Stefan Lange for transcription of the text into the latex language as well as Dorothee Wussow from the University Bibliothek Dortmund for supporting his literature rechearchs. Also he is appreciative to HL-Planartechnik GmbH, giving him the time to write this paper.

APPENDIX: IOFFE-REGEL CRITERION

Let us consider the propagation of an electron with the energy E_F in a disordered homogeneous system characterized by a spherical Fermi surface and a single parabolic band with

$$E_F = \frac{\hbar^2 k_F^2}{2\mathrm{m}}. \tag{A1}$$

Under influence of an electric field a single electron at E_F is accelerated between two successive scattering events covering the path L. The amount of its momentum before and after an elastic scattering event is given by $|p| = (2\mathrm{m}E_F)^{1/2}$ and it follows that the amount of the momentum change during scattering, $|\delta p|$, cannot be larger than $2(2\mathrm{m}E_F)^{1/2}$. In accordance with Heisenberg's uncertainty principle the uncertainties of locality, $\langle \Delta x \rangle$, and momentum, $\langle \Delta p \rangle$, of the electron are determined by[107]

$$\langle \Delta x \rangle \langle \Delta p \rangle \geqslant \frac{\hbar}{2}. \tag{A2}$$

The momentum uncertainty cannot be larger than $|\delta p|$, otherwise the momentum change by scattering would not be defined, i.e.:

$$\langle \Delta p \rangle \leqslant |\delta p| \leqslant 2(2\mathrm{m}E_F)^{1/2} \tag{A3}$$

must be fulfilled. The locality uncertainty, $\langle \Delta x \rangle$, cannot be larger than L, otherwise L would not have a physical sense and with Eqs. (A2) and (A3) it follows $2L(2\mathrm{m}E_F)^{1/2} > \hbar/2$ and with Eq. (A1):

$$k_F L \geqslant 1/4, \tag{A4}$$

i.e., $c^* = 1/4$ (Secs. IV B, IV C, and IV D).

*Electronic address: joachim.sonntag@hlplanar.de

[1] P. P. Edwards, R. L. Johnston, C. N. R. Rao, D. P. Tunstall, and F. Hensel, Philos. Trans. R. Soc. London, Ser. A **356**, 5 (1998).
[2] N. F. Mott, Philos. Mag. **26**, 1015 (1972).
[3] N. F. Mott, Philos. Mag. B **44**, 265 (1981).
[4] E. Abrahams, P. W. Anderson, D. C. Licciardello, and T. V. Ramakrishnan, Phys. Rev. Lett. **42**, 673 (1979).
[5] P. W. Anderson, E. Abrahams, and T. V. Ramakrishnan, Phys. Rev. Lett. **43**, 718 (1979).
[6] D. J. Thouless, in *Anderson Localization*, edited by Y. Nagayoka and H. Fukuyama (Springer-Verlag, Berlin, 1982), p. 2.
[7] W. L. McMillan and J. Mochel, Phys. Rev. Lett. **46**, 556 (1981).
[8] G. Hertel, D. J. Bishop, E. G. Spencer, J. M. Rowell, and R. C. Dynes, Phys. Rev. Lett. **50**, 743 (1983).
[9] S. Okuma, S. Shiratake, A. Asamitsu, and N. Nishida, Solid State Commun. **70**, 1091 (1989).
[10] A. Möbius, C. Frenzel, R. Thielsch, R. Rosenbaum, C. J. Adkins, M. Schreiber, H.-D. Bauer, R. Grötzschel, V. Hoffmann, T. Krieg, N. Matz, H. Vinzelberg, and M. Witcomb, Phys. Rev. B **60**, 14209 (1999).

[11] A. Möbius, D. Elefant, A. Heinrich, R. Müller, J. Schumann, H. Vinzelberg, and G. Zies, J. Phys. C **16**, 6491 (1983).
[12] A. Möbius, H. Vinzelberg, C. Gladun, A. Heinrich, D. Elefant, J. Schumann, and G. Zies, J. Phys. C **18**, 3337 (1985).
[13] A. Möbius, J. Phys. C **18**, 4639 (1985).
[14] A. Möbius, Phys. Status Solidi B **144**, 759 (1987).
[15] A. Möbius, Z. Phys. B: Condens. Matter **80**, 213 (1990).
[16] N. F. Mott and E. A. Davis, *Electronic Processes in Non-Crystalline Materials*, 2nd ed. (Clarendon, Oxford, 1979).
[17] N. F. Mott, *Metal-Insulator Transitions* (Taylor and Francis, London, 1990).
[18] K. Morigaki, Philos. Mag. B **42**, 979 (1980).
[19] N. Kishimoto and K. Morigaki, J. Phys. Soc. Jpn. **46**, 497 (1979).
[20] N. Kishimoto and K. Morigaki, J. Phys. Soc. Jpn. **46**, 846 (1979).
[21] R. Rosenbaum, A. Heines, A. Palevski, M. Karpovski, A. Gladkikh, M. Pilosof, A. J. Daneshvar, M. R. Graham, T. Wright, J. T. Nicholls, C. J. Adkins, M. Witcomb, V. Prozesky, W. Przybylowicz, and R. Pretorius, J. Phys.: Condens. Matter **9**, 5395 (1997).
[22] A. Endo, A. Suzuki, and K. Tanaka, J. Phys. Soc. Jpn. **68**, 3533 (1999).
[23] K. Kawade, A. Suzuki, and K. Tanaka, J. Phys. Soc. Jpn. **69**, 777 (2000).
[24] P. W. Anderson, Phys. Rev. **109**, 1492 (1958).
[25] P. W. Anderson, in *Anderson Localization*, edited by Y. Nagayoka and H. Fukuyama (Springer-Verlag, Berlin, 1988).
[26] J. Sonntag, Phys. Rev. B **40**, 3661 (1989).
[27] In order to avoid confusion, in the following, ζ and β are replaced by ζ_v and β_v, respectively, if they are related to *volume* representation, i.e., $n(\zeta_v)=n_A\exp(-\beta_v\zeta_v)$.
[28] A. M. Edwards, M. C. Fairbanks, A. Singh, R. J. Newport, and S. J. Gurman, Physica B **158**, 600 (1989).
[29] A. M. Edwards, M. C. Fairbanks, and R. J. Newport, Philos. Mag. B **63**, 457 (1991).
[30] R. D. Lorentz, A. Bienenstock, and T. I. Morrison, Phys. Rev. B **49**, 3172 (1994).
[31] M. J. Regan, M. Rice, M. B. FernandezvanRaap, and A. Bienenstock, Phys. Rev. Lett. **73**, 1118 (1994).
[32] M. B. F. van Raap, M. J. Regan, and A. Bienenstock, J. Non-Cryst. Solids **191**, 155 (1995).
[33] S. Yoshizumi, D. Mael, T. H. Geballe, and R. L. Greene, in *Localization and Metal-Insulator Transitions*, edited by H. Fritzsche and D. Adler (Plenum Press, New York, 1985), p. 77.
[34] D. Mael, S. Yoshizumi, and T. H. Geballe, Phys. Rev. B **34**, 467 (1986).
[35] J. Fischer and H. v. Löneysen, Ann. Phys. **2**, 635 (1993).
[36] U. Mizutani, T. Ishizuka, and T. Fukunaga, J. Phys.: Condens. Matter **9**, 5333 (1997).
[37] A. Y. Rogatchev, T. Takeuchi, and U. Mizutani, Phys. Rev. B **61**, 10010 (2000).
[38] K. M. Abkemeier, C. J. Adkins, R. Asal, and E. A. Davis, J. Phys.: Condens. Matter **4**, 9113 (1992).
[39] K. M. Abkemeier, C. J. Adkins, R. Asal, and E. A. Davis, Philos. Mag. B **65**, 675 (1992).
[40] H. Ishii, S. Brennan, and A. Bienenstock, J. Non-Cryst. Solids **299–302**, 243 (2002).
[41] M. J. Regan and A. Bienenstock, Phys. Rev. B **51**, 12170 (1995).
[42] R. L. Rosenbaum, M. Slutzky, A. Möbius, and D. S. McLachlan, J. Phys.: Condens. Matter **6**, 7977 (1994).
[43] P. Mangin, G. Marchal, C. Mourey, and C. Janot, Phys. Rev. B **21**, 3047 (1980).
[44] G. Marchal, P. Mangin, and C. Janot, Philos. Mag. B **42**, 81 (1980).
[45] M. L. Theye, V. N. Van, and S. Fisson, Philos. Mag. B **47**, 31 (1983).
[46] A. J. Shaldervan and N. G. Nakhodkin, Fiz. Tverd. Tela (S.-Peterburg) **11**, 3407 (1969) [Sov. Phys. Solid State **11**, 2773 (1970)].
[47] N. G. Nakhodkin and A. J. Shaldervan, Thin Solid Films **10**, 109 (1972).
[48] F. L. Galeener, Phys. Rev. Lett. **27**, 1716 (1971).
[49] Á. Barna, P. B. Barna, Z. Bodó, J. F. Pócza, I. Pozsgai, and G. Radnóczi, in *Amorphous and Liquid Semiconductors*, edited by J. Struke and W. Brenig (Taylor and Francis, London, 1974), Vol. 1, p. 109.
[50] W. Fuhs, H.-J. Hesse, and K. H. Langer, in *Amorphous and Liquid Semiconductors*, edited by J. Struke and W. Brenig (Taylor and Francis, London, 1974), Vol. 1, p. 78.
[51] P. Thomas, in *Amorphous Semiconductors '76*, edited by I. Kösa Somogyi (Akadémiai Kiadó, Budapest, 1977), Vol. 1, p. 65.
[52] W. Fuhs, in *Amorphous & Microcrystalline Semiconductor Devices*, edited by J. Kanicki (Artech House, Boston, 1992), Vol. II, Chap. Electronic Properties of Amorphous Silicon (*a*-Si:H).
[53] J. C. Knights, in *The Physics of Hydrogenated Amorphous Silicon*, edited by J. D. Joannopoulos and G. Lucovsky (Springer-Verlag, Berlin, 1984), Vol. I, p. 5.
[54] G. S. Cargill III, Phys. Rev. Lett. **28**, 1372 (1972).
[55] R. Messier, S. V. Krishnaswamy, L. R. Gilbert, and P. Schwab, J. Appl. Phys. **51**, 1611 (1980).
[56] E. Davis and N. F. Mott, Philos. Mag. **22**, 903 (1970).
[57] "s^2p^2," "s^2p," and "sp^3" are solely used as symbols of the realized orbital configurations, but not to characterize the occupation [due to electron transfer, Eq. (1)].
[58] K. Kobayashi, F. Itoh, T. Fukunaga, H. Fujimori, and K. Suzuki, in *Rapidly Quenched Metals IV*, edited by T. Masumoto and K. Suzuki (Japanese Institute of Metals, Sendai, 1981), at Sendai, Japan, 24–28 August 1981.
[59] Additional possible amorphous phases between these assumed phases with the composition of *a*-$CrSi_2$ and *a*-$CrSi_3$ seem to be rather unlikely because of several indications: the crystalline counterpart *c*-$CrSi_2$ to a hypothetical *a*-$CrSi_2$-phase has a relatively complex unit cell, and the corresponding SRO is hardly imaginable for an amorphous structure (i.e., without any long-range order), and for *a*-$CrSi_3$ there is not a crystalline counterpart (see Refs. 61–64). Another indication is the result that there is no discontinuity in the slope of the $\lg\rho(\xi)$ dependence on $\xi[\rho=1/\sigma;\xi=x/(1-x)]$, see Fig. 3 of Pap. I.
[60] K. Tanaka, T. Saito, K. Suzuki, and R. Hasegawa, Phys. Rev. B **32**, 6853 (1985).
[61] M. Hansen and K. Anderko, *Constitution of Binary Alloys* (McGraw-Hill, New York, 1958).
[62] F. A. Shunk, *Constitution of Binary Alloys, 2nd. suppl.*(McGraw-Hill, New York, 1969).
[63] G. V. Samsonov, L. A. Dvorina, and B. M. Rud, *Silicides* (Metallurgija, Moscow, 1979).
[64] P. V. Geld and F. D. Sidorenko, *Silicides of the Transition Metals of the Fourth Period* (Metallurgija, Moscow, 1971).
[65] A. Suzuki and K. Tanaka, J. Appl. Phys. **37**, 4872 (1998).
[66] B. W. Dodson, W. L. McMillan, J. M. Mochel, and R. C. Dynes, Phys. Rev. Lett. **46**, 46 (1981).

[67] G. Deutscher, Physica B & C **109 & 110**, 1629 (1982).
[68] Other metastable phases are known for Al-Ge (see Refs. 88 and 108).
[69] G. Deutscher, M. Rappaport, and Z. Ovadyahu, Solid State Commun. **28**, 593 (1978).
[70] D. S. McLachlan, R. Rosenbaum, A. Albers, G. Eytan, N. Grammatica, G. Hurvits, J. Pickup, and E. Zaken, J. Phys.: Condens. Matter **5**, 4829 (1993).
[71] J. Shoshany, V. Goldner, R. Rosenbaum, M. Witcomb, D. S. McLachlan, A. Palevski, M. Karpovski, A. Gladkikh, and Y. Lereah, J. Phys.: Condens. Matter **8**, 1729 (1996).
[72] F. Catalina and C. N. Afonso, Thin Solid Films **167**, 57 (1988).
[73] Y. Lereah, G. Deutscher, and E. Grünbaum, Phys. Rev. A **44**, 8316 (1991).
[74] See Sec. II B of Pap. I and Fig. 2(b) therein.
[75] R. Landauer, J. Appl. Phys. **23**, 779 (1952).
[76] In Secs. IV B and IV C it will be discussed that σ_i at $T=0$ calculated applying the BTE, has only a physical meaning as long as $\sigma_i > (c^*/6)(e^2/h)(1/L_i) \simeq 20\ \Omega^{-1}\ \mathrm{cm}^{-1}$ (for $L_i \simeq d_i$), where d_i is the average atomic distance in the phase i.
[77] B. Abeles, P. Sheng, M. D. Coutts, and Y. Arie, Adv. Phys. **24**, 407 (1975).
[78] B. Abeles, RCA Rev. **36**, 594 (1975).
[79] B. Abeles, in *Applied Solid State Science*, edited by R. Wolfe (Academic, New York, 1976), Vol. 6, p. 1.
[80] S. R. Nagel, Adv. Chem. Phys. **51**, 227 (1982).
[81] W. L. Johnson and A. R. Williams, Phys. Rev. B **20**, 1640 (1979).
[82] Although Eq. (1) is not yet confirmed by independent authors, let us apply the parameter β (or β_v) as a measure for the amount of electron transfer to the phase with the deeper potential.
[83] A. Möbius, Solid State Commun. **73**, 215 (1990).
[84] P. S. Kirejew, *Physik der Halbleiter* (Akademie-Verlag, Berlin, 1974).
[85] T. C. Harman and J. M. Honig, *Thermoelectric and Thermomagnetic Effects and Applications* (McGraw-Hill, New York, 1967).
[86] A. F. Ioffe, *Physik der Halbleiter* (Akademie-Verlag, Berlin, 1958).
[87] D. Elefant, C. Gladun, J. Schumann, and H. Vinzelberg, J. Phys. C **16**, 6491 (1983).
[88] U. Köster, Acta Metall. **20**, 1361 (1972).
[89] The applied value $\beta_v = 1.3$ is to be considered as a grow estimation, since β_v depends on the chosen values for the phase concentrations, x_A and x_B.
[90] G. Hurvits, R. Rosenbaum, and D. S. Mclachlan, J. Appl. Phys. **73**, 7441 (1993).
[91] See, e.g., the TEM-micrografs by B. Abeles *et al.* (see Refs. 77 and 79) for the related class of *cermets* having *granular* structure as well, where such *A*-*A* phase grain contacts (for small x) are visible very well.
[92] Notice that for large x *granular* structure is not realized (see Refs. 42, 70, and 73).
[93] I. Webman, J. Jortner, and M. H. Cohen, Phys. Rev. B **16**, 2959 (1977).
[94] H. Scher and R. Zallen, J. Chem. Phys. **53**, 3759 (1970).
[95] Such a situation was found by Nguyen Van Den *et al.* (see Ref. 109) in a-$(Cr_{0.45}Si_{0.55})_{1-x}O_x$ thin films by ir absorption measurements: in 11 different samples with $x = 0.25 - 0.53$ the dielectric (insulating) oxid phase was found (a) to have a considerable amount of both Cr and Si atoms and (b) the *same structural* unit was realized, independent of x.
[96] M. A. Howson and B. L. Gallagher, Phys. Rep. **170**, 265 (1988).
[97] M. R. Graham, C. J. Adkins, H. Behar, and R. Rosenbaum, J. Phys.: Condens. Matter **10**, 809 (1998).
[98] U. Mizutani and T. Yoshida, J. Phys. F: Met. Phys. **12**, 2331 (1982).
[99] For the Ioffe-Regel criterion $kL \simeq \pi$ (see Ref. 97) or $kL \simeq 1/2\pi$ (see Ref. 110) or $kL \simeq 1$ (see Ref. 16) is given or proposed.
[100] A. Isobe, M. Yamada, and K. Tanaka, J. Phys. Soc. Jpn. **66**, 2103 (1997).
[101] A. Suzuki, A. Endo, and K. Tanaka, J. Phys. Soc. Jpn. **68**, 3623 (1999).
[102] K. Tanaka, K. Furui, and M. Yamada, J. Phys. Soc. Jpn. **64**, 4790 (1995).
[103] Notice that in Refs. 23, 36, 65, and 100–102, x stands for the *metal* concentration, whereas in the present paper x stands for the metalloid concentration as introduced in Pap. I, already.
[104] J. M. Ziman, J. Phys. C **1**, 1532 (1968).
[105] V. K. S. Vinod and S. Kirkpatrick, Adv. Phys. **20**, 325 (1971).
[106] With exception of intermetallic compounds at certain x.
[107] W. Pauli, in *Prinzipien der Quantentheorie I*, edited by S. Flügge (Springer-Verlag, Berlin, 1958), p. 1.
[108] M. Atzmon, C. D. Adams, Y.-T. Cheng, and D. J. Srolovitz, in *Evolution of Thin Film and Surface Microstructure*, edited by C. V. Thompson (Materials Research Society, Pittsburgh, PA, 1991), p. 143.
[109] N. Van Den, A. Heinrich, K. Klostermann, and G. Sobe, Phys. Status Solidi A **93**, 163 (1986).
[110] U. Mizutani, *Introduction to the Electron Theory of Metals* (Cambridge University Press, Cambridge, 2001).